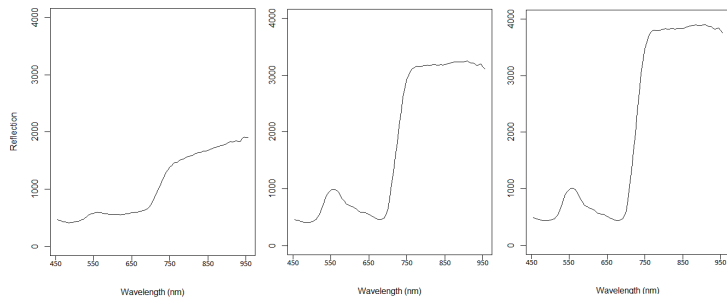# Weed detection with Unmanned Aerial Vehicles in agricultural systems

Thomas M. Koot
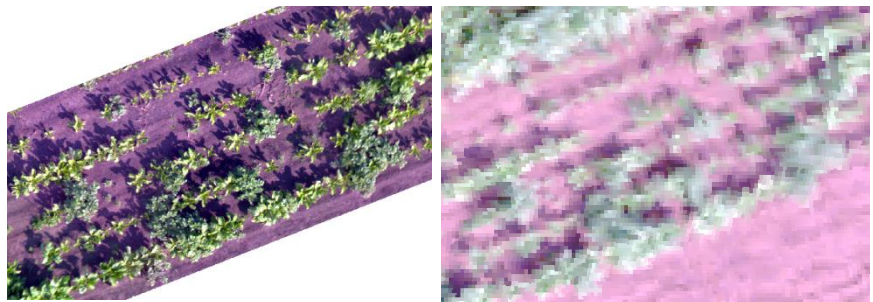
10-12-2014

WAGENINGEN UNIVERSITY
WAGENINGEN UR

Weed detection with Unmanned Aerial Vehicles in agricultural systems

BSc. T.M. Koot

Registration number: 891024465110

Supervisors:
dr.ir. L. Kooistra
dr.ir. J. W. Hofstee

A thesis submitted in partial fulfilment of the degree of Master of Science
at Wageningen University and Research Centre,
The Netherlands.

10-12-2014
Wageningen, The Netherlands

Thesis code number: GRS-80436
Thesis Report: GIRS-2014-37
Wageningen University and Research Centre
Laboratory of Geo-Information Science and Remote Sensing

Acknowledgments

I would like to use this opportunity to express my gratitude to everyone who has supported me during my thesis research, whether by supplying me with help and feedback or by simply drinking some tea with me at times I felt stuck.

Special thanks to my supervisors Lammert Kooistra and Jan Willem Hofstee for continuously providing me with reviews, questions and new ideas. I very much appreciate all the time and effort you have put into this endeavour.

Also many thanks to Juha Suomalainen for operating the UAV and for all the answers to my related and unrelated questions. I enjoyed our trips to the fields.

Summary

This study investigated the potential of using Unmanned Aerial Vehicles (UAVs) in an agricultural weed control system. To do so an UAV is deployed to make aerial RGB and hyperspectral images of three agricultural fields planted with sugar beet plants and volunteer potato plants. Those images are geo-referenced and the hyperspectral images go through several spectral and geometrical pre-processing steps after which they are compressed to multispectral images containing five bands: 440 nm – 510 nm (blue), 520 nm – 590 nm (green), 630 nm – 685 nm (red), 690 nm – 730 nm (red-edge), 760 nm – 850 nm (near infra-red).

Both RGB images and multispectral images have been used to train and validate four classification algorithms: one based on an index (greenness and vegetation for respectively RGB images and multispectral images) and three machine learning techniques: Linear discriminant analysis, quadratic discriminant analysis, Artificial Neural Network (ANN).

The results of the training and validation show that the best classification accuracy (99%) is achieved by an ANN when it is validated on the same field it has also been trained on. When the same classification algorithm is then validated for the two other fields, the classification accuracy drops to 71% and 75%. The same pattern is present for the other tested classification algorithms. This pattern shows that the used classification algorithms are condition sensitive and therefore perform much better on fields they have been trained on than on other fields with the same plants but recorded under different conditions.

Using RGB images as input outperformed the classification where multispectral images were used as input for all tested classification algorithms. However some concerns have been raised on the band choices for the creation of the multispectral images and the use of those bands. Firstly the bandwidths and ranges could have been chosen based on an optimal signal-to-noise ratio and secondly the red-edge band could have been used as a specific wavelength where the red-edge occurs rather than the average reflection value in the red-edge range.

Some propositions are made for a weed control system in which an UAV assists an weed detecting and removing Unmanned Ground Vehicle (UGV) in two different ways: 1. triggering the UGV to go into the field; 2. provide the UGV with an optimum path through the field.

Keywords: weed detection | UAV | crop classification | machine learning | automated weed control

Table of Contents

1   Introduction

1.1   General background

Weed control has been an important and laborious activity since the adoption of modern agriculture. Automation of weed control has proven to be a challenge. While success has been achieved with herbicide resistant genetically modified crops (GM-crops), the use of GM-crops is controversial (Levidow 2001, Levidow & Boschert 2008) and the application of herbicide is ineffective against resistant weeds and volunteer (GM-)crops (Owen & Zelaya 2005).

In the case of regular crops, weeding can be done mechanically before the sowing of the crop or chemically before the emergence of the crop. With mechanical weeding, weeds are generally removed by means of mowing, pulling or burning. Chemical weeding mostly relies on a herbicide that is sprayed on the foliage. Both types of weeding are also possible after the crops are sown and emerged. However, in that case the weeding needs to be location specific, i.e. the location of the weed needs to be known (Zimdahl 2013). Automating the location identification of weeds has been mainly a technological challenge.

For this purpose, earlier studies have explored the potential of unmanned ground vehicles (UGVs) with mounted machine vision, and classification from satellite images (Thorp & Tian 2004). Although the achieved accuracies of identification by machine vision have not always been compelling, the principle seems plausible at least (Hemming & Rath 2001, Nieuwenhuizen et al 2008, Nieuwenhuizen et al 2007). Satellite images however, have had a very limited success due to their often low spatial resolution, sensitivity to atmospheric distortions and low fly-over frequency (Barrientos et al 2011).

1.2   Problem definition

Remote sensing from airborne platforms for weed control has only recently gained more interest, mostly due to the increasing capacities of unmanned aerial vehicles (UAVs) (Zhang & Kovacs 2012). UAVs are flying platforms in the form of unmanned multi-copters or airplanes often with mounted sensors. UAVs have been stated to have a great potential, mainly because they are relatively easy to operate, can be deployed on demand and are able (and often legally limited to) fly close to the ground surface (Xiang & Tian 2011). Although the costs are currently relatively high, it is expected that both the acquisition and operation costs will drop significantly in the near future which would make them applicable for farm scale monitoring (Rango et al 2006).

While UAVs often can record images with a higher resolution (up to cm) compared to satellites, they cannot nearly record their object of interest as close as an UGV could. In spite of not attaining the same resolution, UAVs do have the capacity of recording in a much shorter timeframe than UGVs and can access fields that are not accessible by UGVs. Especially in cases of large fields, a dense crop cover, heterogeneous distribution of unwanted plants and regular monitoring of weeds or pests, using UAVs could be either a great contribution to, or a better alternative than, using UGVs.

The methods of identification for UGVs and UAVs are also different. Although both use the recorded reflection of the plant and of the ground surface, the influence of environmental effects is much more controllable for UGVs. Often UGVs will carry their own light source (Slaughter et al 2008). This means that for UGVs the original spectrum of the light is precisely known, where UAVs can have varying incoming spectra due to atmospheric features, angle of incoming light and local shadows.

UGVs are also much closer to the studied object and often have the possibility to view the object from different angles (Slaughter et al 2008). This has the great benefit that multiple measurements can be taken which cancels the effect of random errors. Sometimes UGVs even create 3D-images of the studied object (Piron et al 2011). These conditions are difficult, if not impossible, to achieve with UAVs.

Studies on weed detection by UGVs mainly focus on the real-time identification of weeds. The purpose of this strategy is the aim for a direct elimination of the weed after being identified. Studies on weed detection by satellites and airborne vehicles often do not focus on a real-time recognition. This is partly

due to the fact that aerial images are pre-processed to eliminate distortions caused by the atmosphere and by tilting of the platform (making the view angle deviate from nadir). Another reason is that satellites and airborne vehicles are not expected to execute an operation after the identification of a weed.

With the introduction of UAVs, however, imaging of weeds can be more on demand and customized during the flight than possible with satellites and more classical airborne vehicles. This means that interactive systems in which ground vehicles communicate with UAVs are now theoretically achievable. For such systems on-board processing on UAVs could become an interesting domain (Ehsan & McDonald-Maier 2009).

Using UAVs for automated weed control, however, brings up a new spectrum of unexplored areas. Such problems range from what kind of sensors to use with what kind of resolution to what kind of algorithms to execute for the identification, and how to incorporate this information acquisition in an agricultural system.

In this study the potential of plant specific identification by UAVs is further explored. In different plots with conventional sugar beet plants, potatoes have been planted to simulate the phenomena of volunteer potatoes; potatoes that were not harvested during an earlier farming cycle and form a weed for the current crop. Potatoes can form a good model system. They are easy to plant, develop to clearly recognisable single plants that are distinct from other cultivated crops. They also form a real threat for many farmers as they do not only compete for resources with the cultivated crop (like general weeds) but have the additional potential disadvantage of transporting pests and diseases (Nieuwenhuizen et al 2007, Shelton & Wyman 1980, Wright & Bishop 1981).

1.3   Objective and research questions

The objective of this study was to assess the possibilities of using UAVs in a weed control system with image-based weed classification. In this study both classification algorithms suggested for UAVs and machine learning classification algorithms used on UGVs were tested for the classification of potatoes and sugar beets on multispectral and RBG images recorded by an UAV on different fields and on different times in the growing season.

This study will also discuss the benefits of including weed classification by UAVs and the challenges for both recognition and real-time processing of the acquired images.

In this way the study aimed to answer the following questions:
1. To what extent and with what kind of image-based identification method could volunteer potatoes and sugar beets be identified?
2. How does classification by indices perform compared to machine learning algorithms?
3. What are the potentials of weed recognition by UAVs?
4. To what extent is real-time recognition by UAVs feasible and what could be the potential applications?

2 Literature review

2.1 History of modern weed control

Weeds in agricultural systems form an important constraint for the health of agricultural crops and both the quality and quantity of the harvest. This constraint is mainly caused by the competition for resources like nutrients, water and sunlight between the crops and the weeds (Nieto et al 1968, Zimdahl 1980). Although weed control can be assumed to be an integral part of agriculture ever since its invention, weed control as a defined practice has been found in literature for about 800 years. However specific mechanical devices for weed removal were mostly adopted in the 20th century while modern chemical weed removal only came into existence in the 1940s (Timmons 1970).

With the aid of tractors and ploughs the complete removal of all growing plants on a particular field has become a relative easy execution and can be performed before the seeding of the crops. However, once crops are developing, any removal of plants needs to exclude the crop itself. In the absence of a mechanical solution for such a plant specific weed control, the vast majority of conventional agriculture either has refrained itself from selective weed removal or has adopted the use of herbicides in combination with herbicide tolerant crops (Kudsk & Streibig 2003).

The use of herbicides has raised some significant concerns which include:

1. The use of herbicides has been linked to environmental damage and negative effects on human health (Weisenburger 1993);
2. The use of herbicide tolerant crops, especially when created by genetic modification has led to resistance from environmentalists and the general public (Singh et al 2006, Wynne 2001);
3. The use of herbicides has caused a lot of weeds to develop resistance towards herbicides which makes this form of weed control becoming less effective over time and imposes dangers for natural ecosystems (Duke 2005, Goldburg 1992, Kudsk & Streibig 2003, Radosevich et al 1992).

Those concerns call for feasible alternatives for, or strong reductions in, chemical weed control. Plant specific weed control is already being used but it does require the investment of a lot of human labour and is currently limited to organic agricultural systems. In order to automate the process of physical weed removal the desired crops and the other (undesired) plants need to be successfully identified (Ghazali et al 2008).

2.2 Weed detection in agricultural systems

Weed detection has recently gained more interest from scientific research. Much of this research has focused on the potential of weed detection in agricultural systems that use herbicide for weed control. In those cases weed maps are used for spatial variable herbicide application (Feyaerts & Van Gool 2001, Gerhards & Christensen 2003, Perez et al 2000, Vrindts et al 2002).

In the case of Feyearts and Van Gool (2001) the weed detection is performed with an UGV equipped with both a RGB sensor and a herbicide spray nozzle. The RGB values are used to calculate a normalized difference vegetation index to distinguish crops, in their case sugar beets, from weeds. (Feyaerts & Van Gool 2001)

In the study of Perez, et al. (2000) images of cereal fields are used to calculate the NDI and from that the shape of the leaves. This information is used by a Bayesian rule classification algorithm and a k-Nearest Neighbour algorithm to distinguish cereal plants from weeds (Perez et al 2000).

In the study of Vrindts, et al. (2002) a different approach is taken. Here hyperspectral cameras are used to identify the hyperspectral signatures of several crops, in their case sugar beets and maize, and several common weeds. They then select the wavelengths that are proofed to be significant for identifying their chosen crops and weeds and use those wavelengths as classifiers (Vrindts et al 2002).

While creating weed maps can significantly reduce the herbicide usage, up to 60% for herbicides against broad-leave weeds and 90% for herbicides against grass weed herbicides (Gerhards &

Christensen 2003), the risk of false positives (crops identified as weed) is limited to the unnecessary use of extra herbicide.

When it comes to physically removing weeds the risk of identifying the crop as a weed or not being able to identify the exact location of the weed is much larger. Even small percentages of false positives would entail unacceptable reductions in potential harvest. This may help to explain why most autonomous weed control UGVs have been calibrated to have false positive percentages as low as 1% but have false negatives (weeds that are not identified as weed) ranging from 16% to 59% (Slaughter et al 2008).

So far the vast majority of research has been focused on the potentials of weed detection by UGVs. Although weed detection from aerial sensors is not unprecedented, most of the earlier studies have focused on mapping weed intensities often in a rather coarse resolution (Lamb & Brown 2001, Pudełko et al 2008). With the increasing potentials of UAVs there has been some research on the possibility of location specific weed identification by aerial vehicles flying on low altitudes (Torres-Sánchez et al 2013).

UAVs could contribute to weed control by making weed maps used for herbicide spraying or doing regular monitoring and trigger a weed removal process when a certain weed limit is exceeded. When real-time , or semi real-time, classification is integrated in the system, the UAV could assist an UGV by pre-selecting probable weeds. This gives the UGV a possibility to do optimum path planning which could save both time and consumed energy (Hansen et al 2013, Kazmi et al 2011). Despite such applications, specific results and analysis of effective identification algorithms by UAVs are largely missing.

2.3 Classification algorithms and approaches

UGVs can come closer to the plants, are often able to take images from different angles and have the ability to carry their own light source. Because several environmental factors are controlled, this allows different classification methods that are more sensitive to their input images.

For crop and weed identification by UAVs, spectral vegetation indices have been suggested as a basis to make the classification between soil, crop and weed. When an infrared-band is available this could be a vegetation index, when the input just consists of RGB images a greenness index has been proposed (Torres-Sánchez et al 2013). In the study of Torres-Sánchez et al. (2003) an UAV is used to record RGB and multispectral images of fields with sunflowers and unspecified weeds on different altitudes. From those images three indices, the NGRI, the ExG and the NDVI, have been computed (Figure 1). The results of this study clearly show that the values of the indices do differ for different altitudes and that based on the used indices it is not always possible to separate the crop from the weed.

Some studies have suggested to apply weed detection by object based classification. In this type of classification the form and structure of the plant (or attributes of the plant like the leaves) are used for determining its type (Lee et al 1999, Shinde & Shukla 2014).

Another option is to do the classification based on reflection by applying machine learning techniques. Machine learning is a method of programming computers to find rules and patterns in data. These rules and patterns can then be used for taking decisions (McQueen et al 1995).

There have been several studies on UGVs running a machine learning algorithm for the classification of weeds. Some studies and their results are shown in Table 1. These studies have been performed under different circumstances and with different crops and different methods. The study of Cho et al. (2002) used RGB images to find crop characteristics like leaf shapes. These features were then used in a discriminant analysis and in a neural network to classify weeds, in their case Purslane, crabgrass and goosefoot (Cho et al 2002). In the study of Jafari et al (2006), a stepwise discriminant analysis was used in which the RGB reflection values were used to come to a classification. In their case weeds consisted of a unspecified mixture of unwanted plants and grasses (Jafari et al 2006). In the case of Piron et al.

(2011) stereo sensors are used to estimate the height of the plants in their images. A quadratic discriminant analysis is then used to try to separate the unspecified mixture of weeds from the carrot plants (Piron et al 2011).

Because of the different crops, sensors and plants used in these studies, the listed accuracies are not necessarily directly comparable. On the other hand, they do give an indication of the current methods for crop classification and there accuracies.
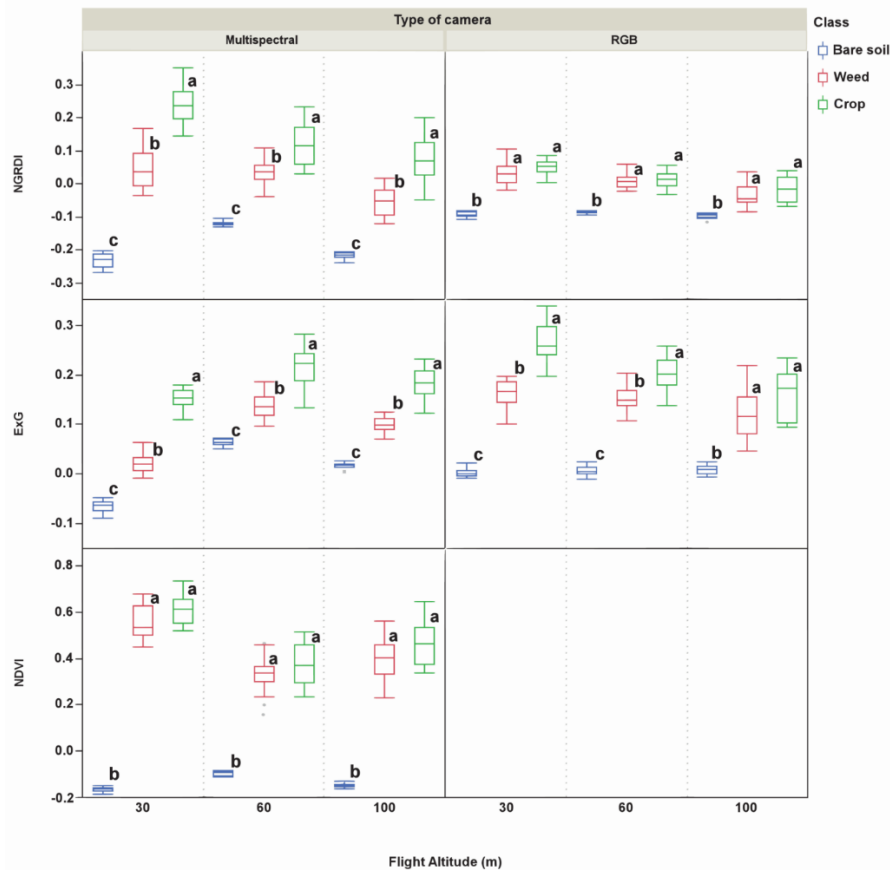
Figure 1. Difference in vegetation index values for bare soil, weed and crop from UAV image data on different altitudes for three indices: NDVI, ExG, NGRDI. Within a group, box-plots followed by the same letter do not differ significantly (taken from Torres-Sánchez et al., 2013).

Table 1. Weed detection algorithms and identification accuracies by machine vision with images from UGV

Algorithm (for crop and weed identification)	Sensor	Crop	Accuracy of weed detection	Misclassification of crops	Source
Discriminant analysis	RGB-sensor	Radish	98%	8%	(Cho et al 2002)
Artificial Neural Network	RGB-sensor	Radish	100%	0%	(Cho et al 2002)
Discriminant analysis	RGB-sensor	Sugar beet	90%	22%	(Jafari et al 2006)
Quadratic discriminant analysis	Stereo (3D) sensors	Carrots	57% - 80%	15% - 25%	(Piron et al 2011)

3   Methodology

This study describes the process of testing various algorithms for weed detection, specifically for volunteer potatoes in a sugar beet field. The process can be divided in several steps (Figure 2). In this chapter the methodology for every step is elaborated on.

- • Planting of potatoes

- • Image acquisition

- • Preprocessing

- • Ground truth extraction

- • Creating training and validation sets

- • Testing the selected algorithms for classification
- • Testing the impact of training on the results
- • Deriving hyperspectral signatures from hyperspectral images
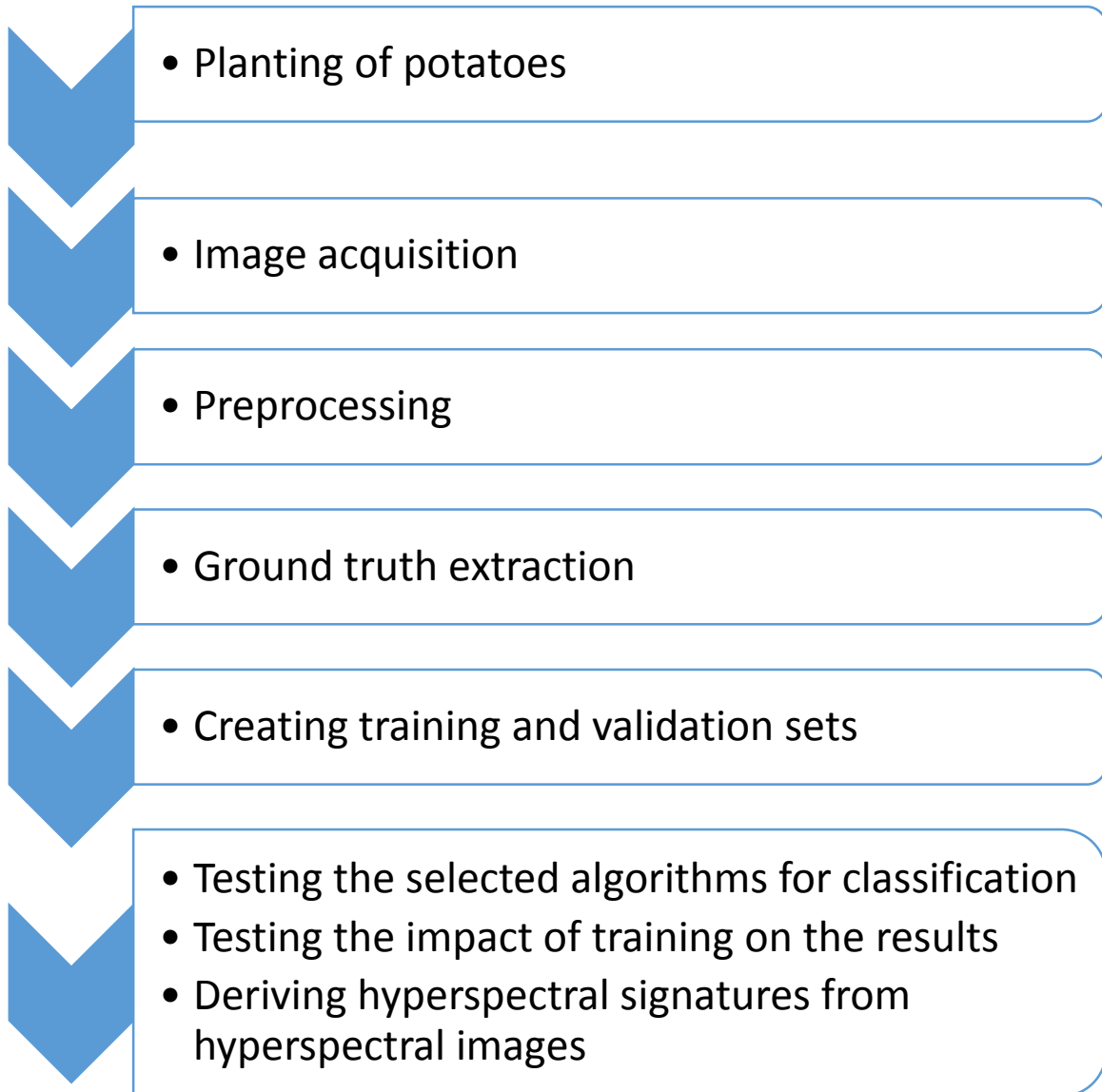
Figure 2. Flow chart of the research methodology

3.1   Planting and field conditions

The potatoes and sugar beets have been planted in two stages during the summer of 2013 (Table 2). The planting took place on three experimental fields (Figure 6) owned by Wageningen University.
The sugar beets were planted by a conventional precision planter with standard row distance (50 cm), and intra row distance. The potatoes were then planted by hand. There was no grid predefined for the plantation of the potatoes nor were their locations recorded. Instead the potatoes were manually semi-randomly distributed over the field.
On the date of the image acquisition on field 1 both the potatoes and sugar beet plants were already well developed (Figure 3). Much less developed were the potatoes and sugar beet plants at field 2 on the date of acquisition. This is presumably due to their later planting date and therefore less optimal

growing season (Table 2). On the date of image acquisition the atmosphere was cloudy and the soil rather wet (Figure 4).

The development of the sugar beet plants and potatoes at field 3 on the date of the acquisition was in between those on field 1 and 2 (Figure 5). Compared to the other fields, the potato and sugar beet plants on field 3 had however the shortest growing period (Table 3). The atmosphere was mostly clear with an exception of some high cloud formations on the date if the image acquisition.

Table 2. Setup of experimental fields

Field nr	Sowing date sugar beets	Planting date potatoes	Main soil component	Date of acquisition
1	26th of July 2013	2nd of August 2013	Sand	13th of September 2013
2	3rd of September 2013	9th of September 2013	Clay	23th of October 2013
3	1st of May 2013	8th of May 2013	Sand	16rd of June 2013

Table 3. Growing days of crops at date of image acquisition

Field nr	Growing days sugar beets at image acquisition	Growing days potatoes at image acquisition
1	45	41
2	50	44
3	38	30

Figure 3. Field 1 (between the dotted lines) on date of image acquisition
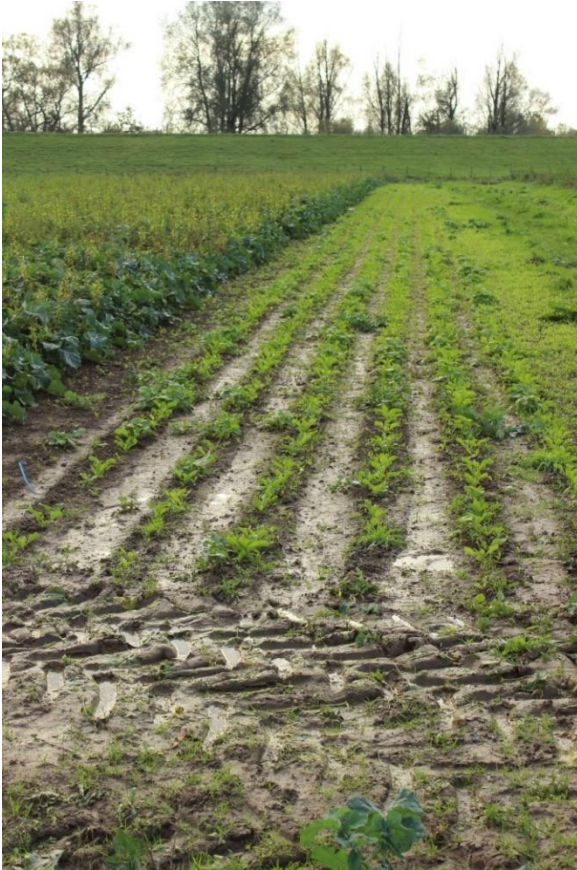
Figure 4. Field 2 on date of image acquisition

Figure 5. Field 3 on date of image acquisition

3.2 Image acquisition

The images of the experimental fields were made by a RGB sensor (Panasonic GX1) and a hyperspectral sensor (PhotoFocus SM2-D1328 + Specim ImSpector V10 2/3) mounted on an octocopter. The used octocopter is an electrically driven UAV that can carry payloads up to 2 kg (Suomalainen et al 2014). The acquired images were used to derive three products: a georeferenced orthomosaic created from the RGB images, a georeferenced hyperspectral image created from the recorded reflection of the hyperspectral sensor and a digital surface model that shows the elevation of the surface (including the

8

elevation of vegetation) created from the RGB images and the recorded orientations of the UAV during the flight (Suomalainen et al 2014). The first two products were used in this study.

Figure 6. Three experimental 'sugar beet - potato' fields around the city of Wageningen which have been used in this study (Table 2)

During all flights the octocopter recorded the imagery from an elevation of 16 meter recording elevation. At this height and with the equipment used during the acquisition, the pixel resolution of the RGB images is about 4 mm while the pixel resolution of the hyperspectral images varied around 6 cm (Figure 7).

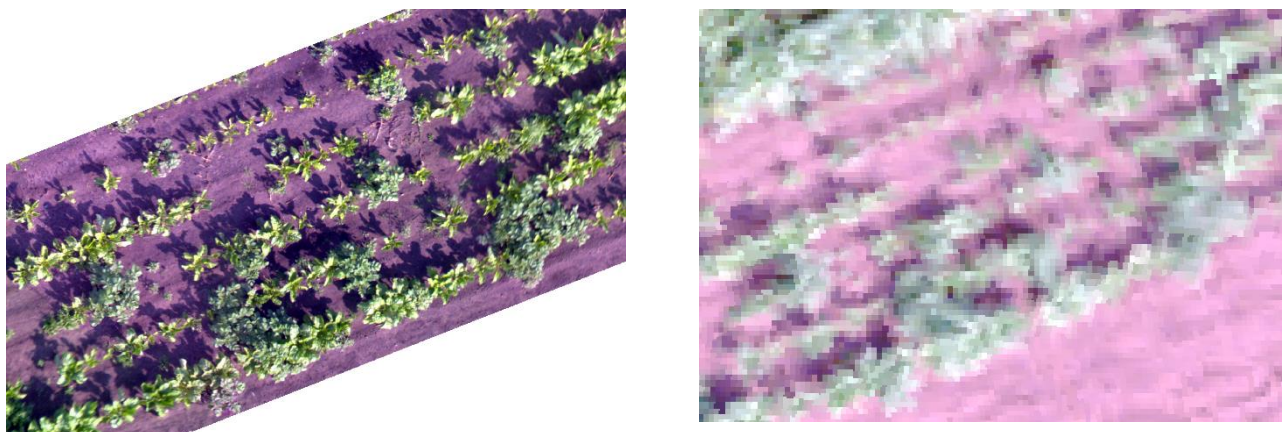**Figure 7. RGB image (left) and hyperspectral image (right) representing 450 nm as blue, 520 nm as green and 650 as red of part of field 1**

9

3.3   Image pre-processing

The pre-processing chain started with converting the raw hyperspectral images from digital numbers to radiance units. As a following step the spectral resolution is resampled. The original sampling of the hyperspectral camera was around every 3 nm but varies slightly. During the resampling the images were resampled to steps of 5 nm by use of a Gaussian Filter. The last step of the spectral processing was the conversion from the radiance units to a reflectance factor by use of a reference panel (25% Spectralon) that has been photographed prior and post every flight (Suomalainen et al 2014).

After the spectral processing the images have been geometrically processed. The RGB images were also mosaicked to form one complete picture. The geometrically processing used the UAV's on-board GPS-ins, the ground control points and the recorded camera orientations during the flight to interpolate the location of every pixel in the images (Suomalainen et al 2014).

Despite this pre-processing chain, the resulting hyperspectral images were not yet useable as such. This is mainly due to the low flying height and therefore high resolution of the images. Especially the local geometric distortions due to the tilting of the UAV caused some locations to deviate from the locations recorded by the RGB camera. Because of the hyperspectral images crop lines that were supposed to be straight showed peculiar curves at some locations on the multispectral images it was a given that it were indeed those images that needed a correction. To improve this a manual triangular warping (Glasbey & Mardia 1998) has been applied, using the software packages of Erdas Imagine 2014. In this method ground control points (gcp's) are defined both in the hyperspectral images and in the RGB images. The hyperspectral images were then warped over the RGB images where triangular interpolation was used for interpolating the location of pixels between the gcp's (Figure 8). For every field about 140 gcp's have been used. These gcp's were centred mainly around significant distortions. During this transformation the original resolution has been maintained.
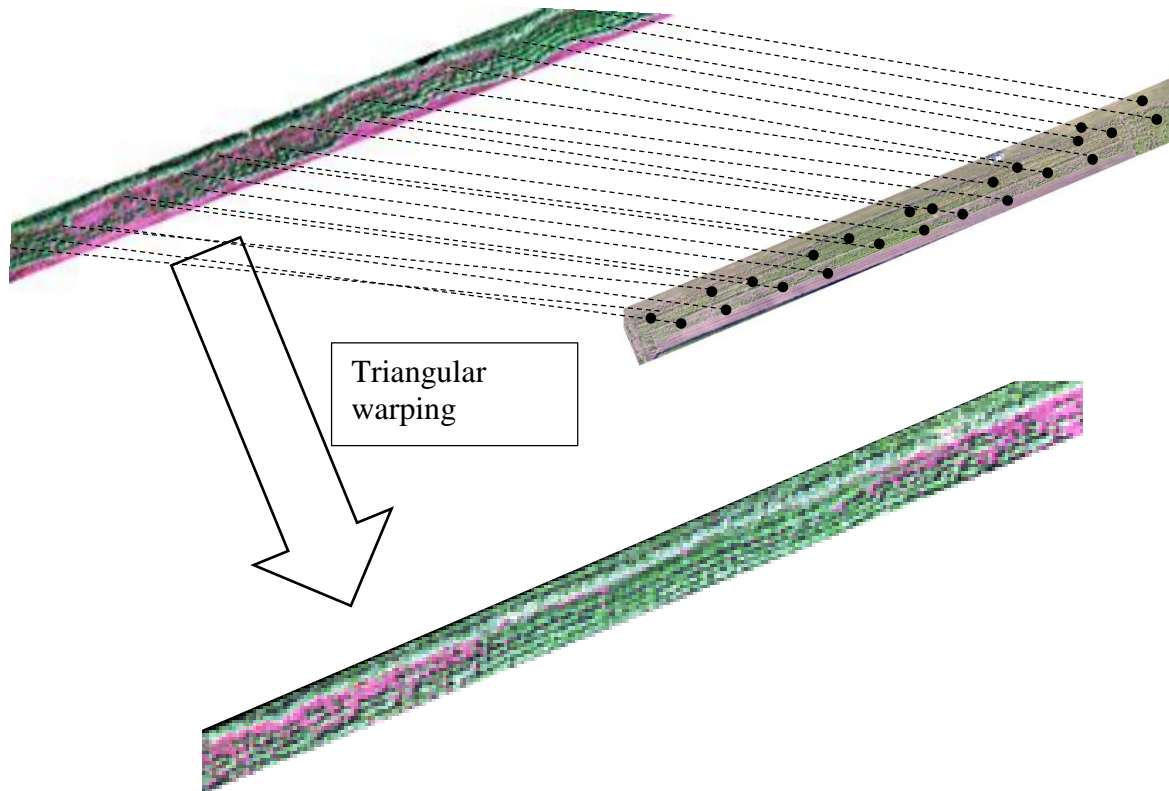

Triangular warping

Figure 8. Using gcp's and RGB image to warp hyperspectral picture

The resulting hyperspectral images were then transformed to a multispectral image that included the RGB bands plus a red-edge and a NIR (Near-Infrared) band (Table 4). The bands used for the creation of the multispectral images are based on bands in the RapidEye satellite (Tyc et al 2005). The values given to those bands consist of the average reflection value recorded in those respective bandwidth ranges. This transformation reduced the number of input bands (from 100 to 5). With that transformation the size of the input images and the computational demand of the algorithms is significantly reduced while the original resolution stays unaltered. With the current state of technology this seems a necessary step to enable the possibility of real-time identification.

The resulting multispectral images have a NIR band included because this band is often used (in relation to the red band) for vegetation identification (Elvidge & Chen 1995). The red-edge band has been included as the red edge in some cases could be quite distinct for various vegetation species (Elvidge & Chen 1995, Miller et al 1990).

Table 4. Bands used for the creation of the multispectral images

Band	Bandwidth range
Blue	440 – 510 nm
Green	520 – 590 nm
Red	630 – 685 nm
Red Edge	690 – 730 nm
Near Infra-Red	760 – 850 nm

3.4 Ground truths extraction

On the RGB images, patches have been defined that belong to either of the following categories:
1. Bare soil
2. Sugar beet plant
3. Potato plant

Those patches were manually drawn and fall within the borders of a plant or bare area. Mixed pixels and pixels belonging to another category are thus avoided. The size of those patches ranges from 0.01 m² to 0.2 m². Furthermore, a single patch never covers more than one plant. The selection of the patches is performed in ArcMap 10.2. The drawing of patches is done by the creation of polygons on the location of a selected patch.

Those patches are later used to extract a mean value for all band reflections. Hence for the RGB image extraction every patch gets three values and for the multispectral image a copy of the same patch gets five values.

The acquired ground truth samples have been divided into two groups (Figure 9). The first group is the training dataset which consists of half of field 1 containing 447 samples. The second group is the validation dataset which consist of the samples of the other half of field 1 and the samples of field 2 and 3, containing all together 1487 samples. This procedure is executed both for the RGB images and the multispectral images.

| Training group | Validation group |

First half of Field 1   Second half of Field 1

Field 2

Field 3
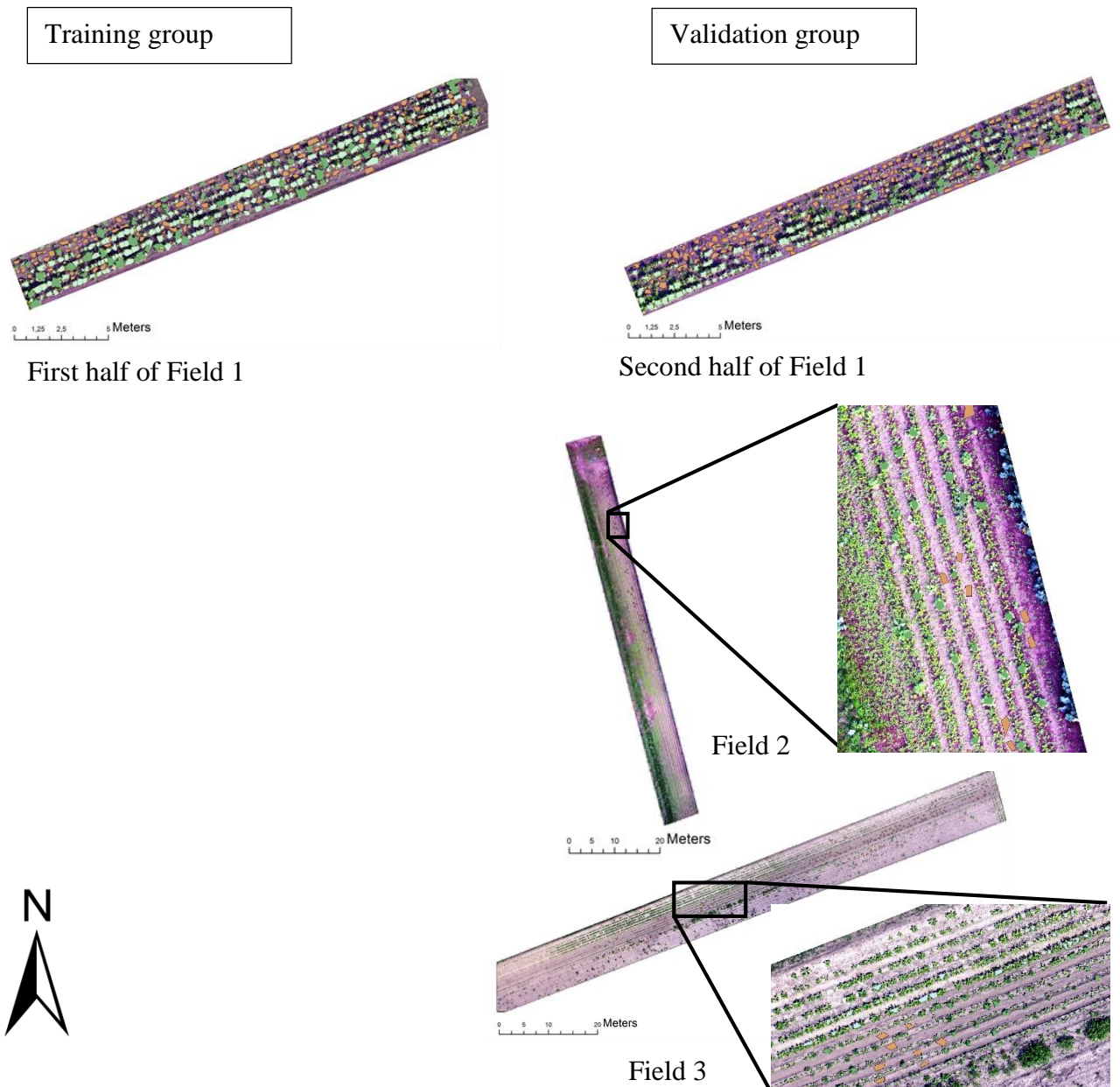
Figure 9. Location of training and validation samples for evaluation of classification algorithms

3.5   Scripting

The actual analysis is being executed in RStudio running a R 3.1.0 version. To access the reflection information the R-package 'Raster' is used. This package allows for extracting the values of a raster. To get instead the reflection of the previous identified patches the earlier created polygons were used to mask the original raster, in this case a RGB or multispectral image of one of the fields. Applying such a mask resulted in a list of reflection values below every polygon. Those lists were then averaged to three (Red, Blue, Green) and five (Red, Blue, Green, Red-edge, NIR) values per patch.

This value extraction resulted in two datasets (a RGB and a multispectral) per field and four datasets for field 1 since this field has been divided in a training and a validation part. Every dataset consisted of the averaged reflection values for every patch. Every patch was also tagged with the class it belongs to.

For every processing step some code has been written. This code needed to be able to read the dataset and apply the specific algorithms on them. In the case of the indices, that code also needed to be able to find the optimal threshold which results in the best classification accuracy on the training dataset. In case of the machine learning techniques the algorithms were already coded in predefined packages.

In those cases code needed to be written to transform the datasets to a form that can be fed to those packages. Finally the result of every algorithm needed to be written to result files.

3.6 Classification algorithms

To identify the potentials of weed classification by UAVs this study trained and validated several algorithms. In earlier literature, the use of simple indices was already proposed for weed classification by UAVs. Two of them, a greenness index and a vegetation index, were tested here.

To compare this with more complicated machine learning algorithms, often used by the current UGVs, this study assessed all the machine learning techniques listed in Table 1. The input for those machine learning techniques consisted of just the reflection values identified from the RGB and multispectral images. Attributes like the height of the plants, the structure of the plants and the form of the leafs were not taken into account.

The result of each classification algorithm is presented in a graph depicting the classification accuracy of this algorithm per field and per class of a certain field. The accuracies per class of a certain field show a percentage of true positives achieved for those classes in that particular field. Those accuracies were then averaged to classification accuracies per field. Finally for every algorithm the accuracies of the fields were averaged to get an indication of the performance of that particular algorithm as a whole.

3.6.1 Greenness index classification

Using the greenness as a way of discriminating plants from soil and of classifying plant themselves is an intuitive method. Instead of looking at the absolute green reflection value, most studies use a weighted value. Based on previous results, in this study a green reflection value was used that was divided by the total VIS reflection (Westergaard-Nielsen et al 2013):

$$Relative\ greenness = \frac{Green}{Red + Green + Blue}$$

The greenness index classification is only tested on RGB images as more bands do not contribute to the result of the used formula. The thresholds (Table 5) have been determined by finding the threshold that results in the optimal classification result for the training group. This threshold was then also applied to the validation group.

Table 5. Optimal thresholds for classification using a greenness index

Class	Relative greenness value range
Soil	$0 - 0.39$
Potato plant	$0.39 - 0.44$
Sugar beet plant	> 0.44

3.6.2 Vegetation index classification

A vegetation index is often used for identifying vegetation and for identifying characteristics of that vegetation. The most commonly used vegetation index is the NDVI (Normalized Difference Vegetation Index) (Crippen 1990):

$$NDVI = \frac{NIR - Red}{NIR + Red}$$

The vegetation index classification is only tested for the multispectral images as the RGB images do not contain a NIR-band. The thresholds (Table 6) have been determined by finding the threshold that results in the optimal classification result for the training group. This threshold is then also applied to the validation group.

Table 6. Optimal thresholds for classification using a vegetation index

Class	Vegetation index value range
Soil	$0 - 0.52$
Sugar beet plant	$0.52 - 0.77$
Potato plant	> 0.77

3.6.3   Linear discriminant analysis

Somewhat similar to predicting the class of the patch by an index with a certain threshold is predicting the class by use of a Linear Discriminant Analysis (LDA). A LDA is trained on classes with a set of values belonging to those classes. In this case the LDA is trained on all reflection values that are attached to a certain patch. Based on the distribution of band values of every separate class a predictor is created. This predictor contains thresholds for all included bands (Venables & Ripley 2002). So for a RGB image the predictor will assign a separate red, green and blue threshold for the class 'soil', 'potatoes' and 'beets'. Thus it takes all available information into account.

For the LDA classification both the RGB and the multispectral images are used. In the latter case also the red-edge and the NIR band was taken into account.

3.6.4   Quadratic discriminant analysis

The Quadratic Discriminant Analysis (QDA) is equal to the LDA with the difference that the QDA does not assume the covariance between the classes is the same (Venables & Ripley 2002). This means that if for example green and blue are very correlated for beets and potatoes, the QDA does not assume the same degree of correlation for patches of soil.

Like for the LDA classification, for the QDA classification both the RGB images and the multispectral images are used.

3.6.5   Artificial Neural Network

Artificial Neural Networks (ANNs) are models that resemble the computations done by a nerve system. An ANN comes with a number of simple artificial nodes that form a network. Prior to training an ANN all the nodes get assigned a weight which determines if they pass a signal of a certain strength through or not. During the training those weights are then adjusted to form a network with the highest predicting accuracy (Venables & Ripley 2002). The initial values for these weights can however lead to a local rather than a global solution. Running an ANN multiple times can therefore create different results (Pollack 1990). In this study the neural network will be executed ten times. The results are the average of those separate results.

An ANN also needs to be initialized with a number of hidden layers (Venables & Ripley 2002). The actual number of hidden layers used here was determined by which number results in the highest classification accuracy during the calibration.

For the ANN classification both the RGB and the multispectral images were used. In the latter case also the red-edge and the NIR band were taken into account.

3.7   Hyperspectral signatures

To get a better understanding of classification accuracies achieved by the described algorithms and to analyse possible improvements, the reflection values for the different classes (sugar beet plants, potato plants and soil) are depicted for the three fields. For the RGB images a boxplot was used to show the reflection values for those classes.

The reflection recorded by the hyperspectral camera are shown as a hyperspectral signature. This is a line graph where the reflection values are plotted against the wavelength of that recorded value. In this case the plots show both the average reflection values and the lower and upper quartile.

Those graphs allow a visual assessment of the differences in reflection between the various classes and between the various fields. Since in this study the hyperspectral data has been compressed to

multispectral data consisting of 5 bands, the hyper spectral signatures also show the reflection that has not been taken into account in the analysis.

4 Results

The results of this study are threefold. First of all the classification accuracies achieved by the algorithms are presented including an elaboration on the performance of every algorithm separately. Secondly the impact of training an algorithm under specific conditions is tested by training two algorithms (LDA and QDA) also on field 2 and validating it on the other fields accordingly.

Thirdly, the average reflection of the sugar beet plants, potato plants, sand soil and clay soil are presented for both the RGB-images and the hyperspectral images.

All graphs are made from the classification matrices (Appendix A) produced by every algorithm for every field. Appendix A also shows the false positive classifications for all classes.

4.1 Validation of classification algorithms

4.1.1 Greenness index
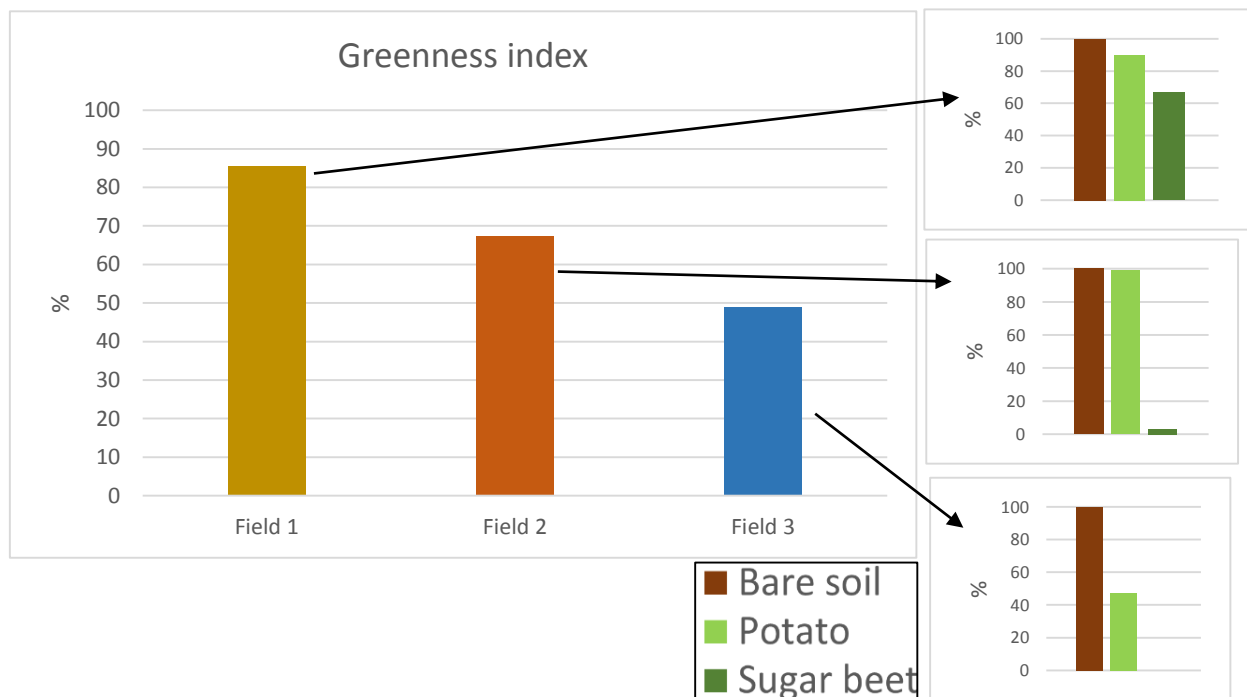
Figure 10. Classification results for greenness index

The results of the greenness index (Figure 10) show that this algorithm identified all soil patches correctly. The thresholds that have been established by training the greenness index on half of field 1 work well in terms of identifying beets and potatoes in the other half of field 1. However these thresholds (Table 5) prove to be unsuccessful in identifying beets and potatoes in field 2, where most of the beets were recognized as potatoes, and field 3, where about half of the potatoes were recognized as beets and all of the beets were recognized as potatoes. All together the classification accuracies average to 67%.

4.1.2 Vegetation index

The results of the vegetation index (Figure 11) show a similar pattern as the results from the greenness index. Like the greenness index, the vegetation index excels at separating soil from vegetation, although this holds here only for field 1 and 3. Also the vegetation index often seems to recognise beets as potatoes and vice versa, especially on the plots it has not been trained on.

All together the classification accuracies average to 61%.
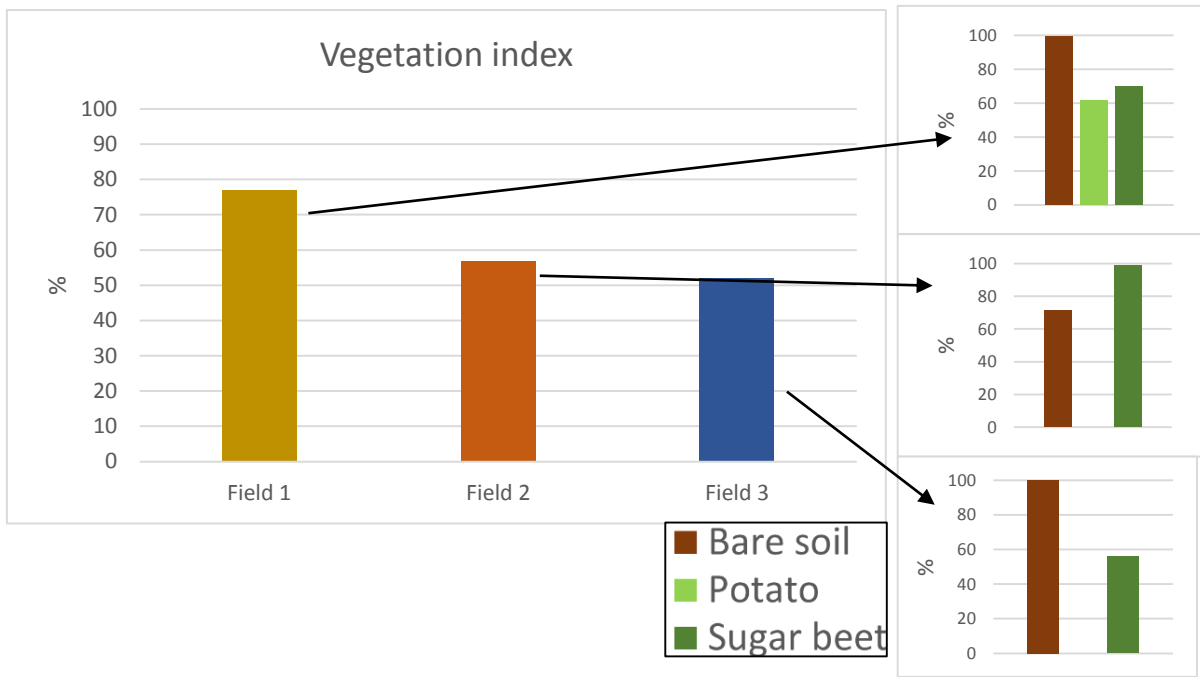
Figure 11. Classification results for vegetation index

4.1.3 Linear discriminant analysis

The linear discriminant analysis (Figure 12) has a high prediction accuracy on field 1 (the field it has been trained on), both for the RGB images as the multispectral images. Like with the greenness and vegetation index, the linear discriminant performs poorly on the other fields mostly because it does not seem able to accurately recognise beets from potatoes and vice versa.

All together the classification accuracies for the RGB images average to 87% and for the multispectral images to 68%.
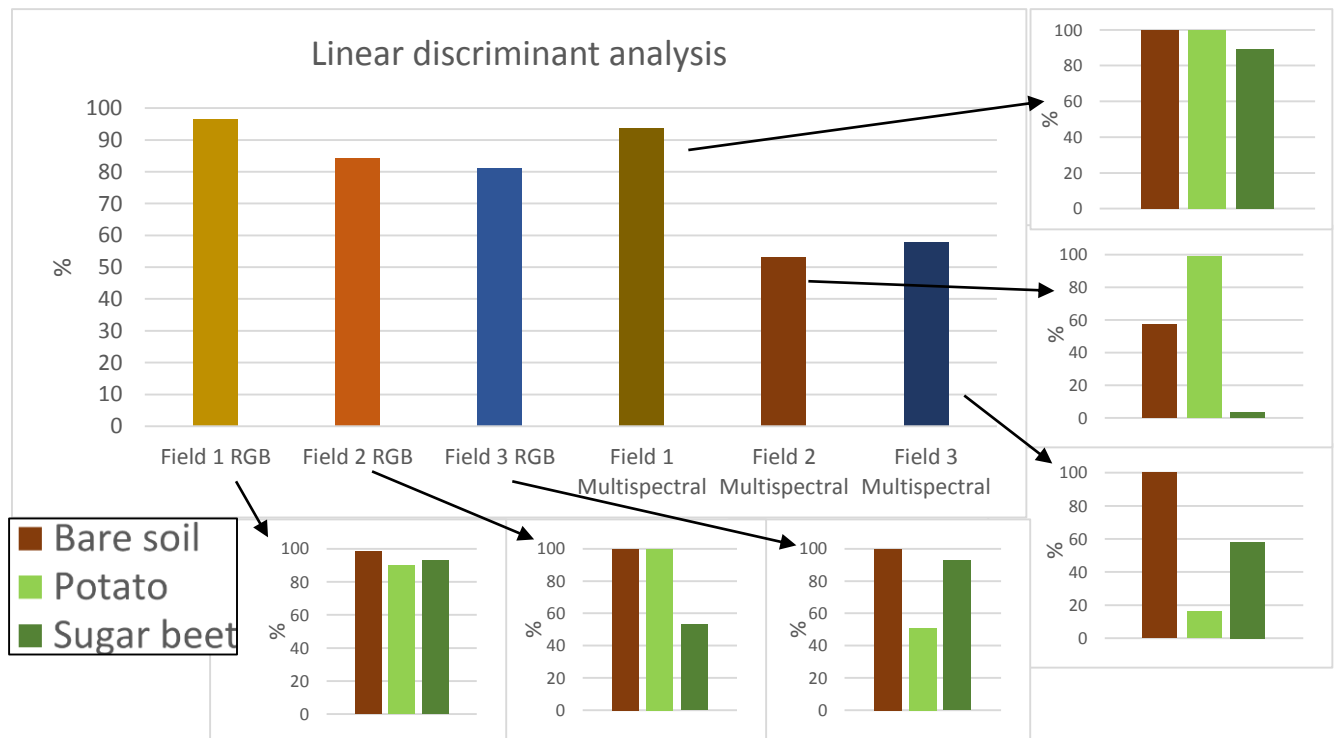
Figure 12. Classification results for linear discriminant analysis

4.1.4 Quadratic discriminant analysis

The quadratic discriminant analysis (Figure 13) also performs well on the field it has been trained on but much poorer on the other fields. The errors are similar to the errors made by the linear discriminant analysis.

All together the classification accuracies for the RGB images average to 75% and for the multispectral images to 61%.
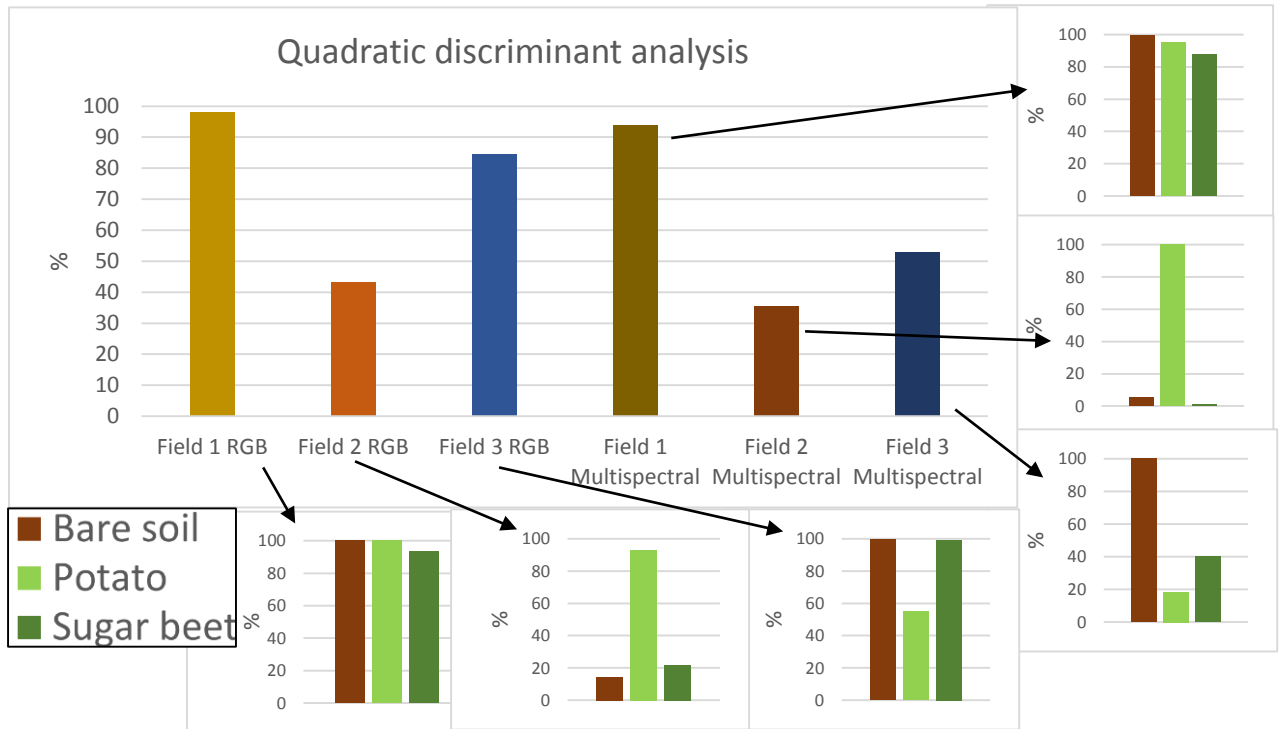
Figure 13. Classification results for quadratic discriminant analysis

4.1.5 Neural network
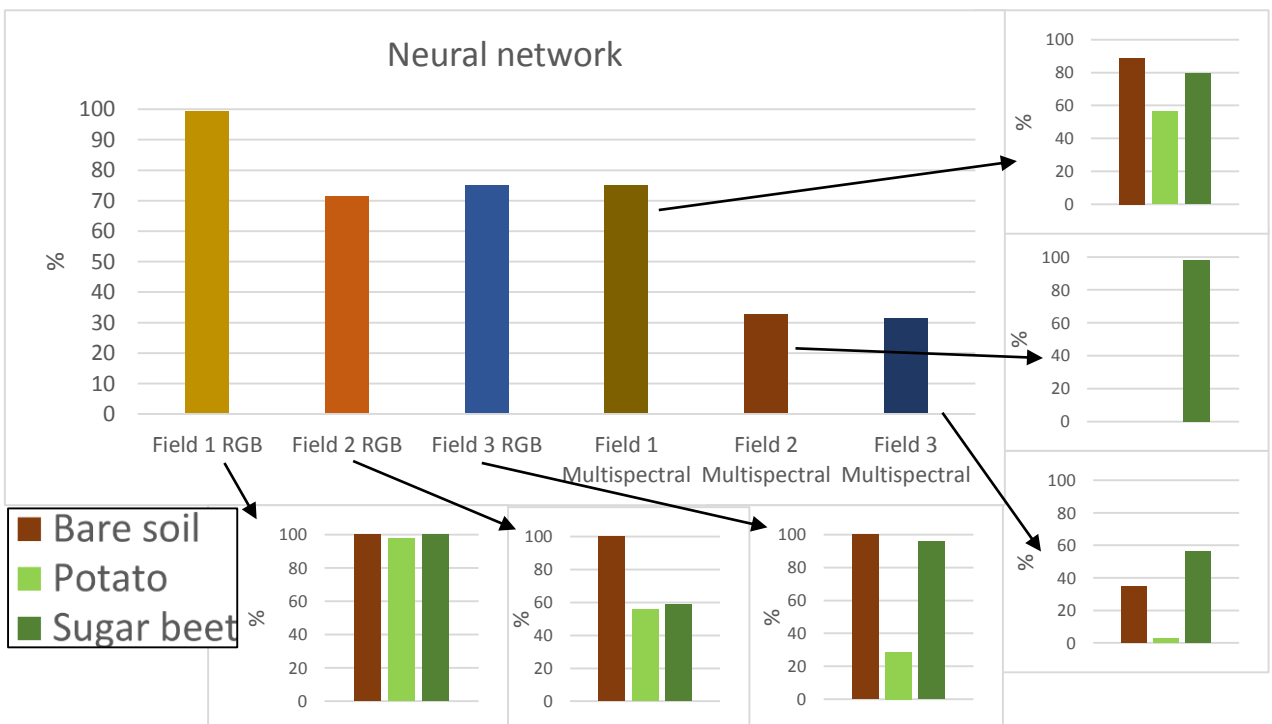
Figure 14. Classification results for neural network

The neural network (Figure 14) achieves by far the best results on the RGB image of field 1 with a classification accuracy of 99.1%. For the fields it was not trained on its performance is much worse. Unexpectedly, training a neural network on the multispectral image of field 1 does not yield a nearly as high classification results as training it on just the RGB image.

All together the classification accuracies for the RGB images average to 82% and for the multispectral images to 46%.

4.1.6   Overall accuracies

The overall accuracies show that the linear discriminant analysis achieves the highest classification accuracy for both RGB images and multispectral images. The results also show that for all used algorithms the classification accuracies are higher when RGB images were used as input.
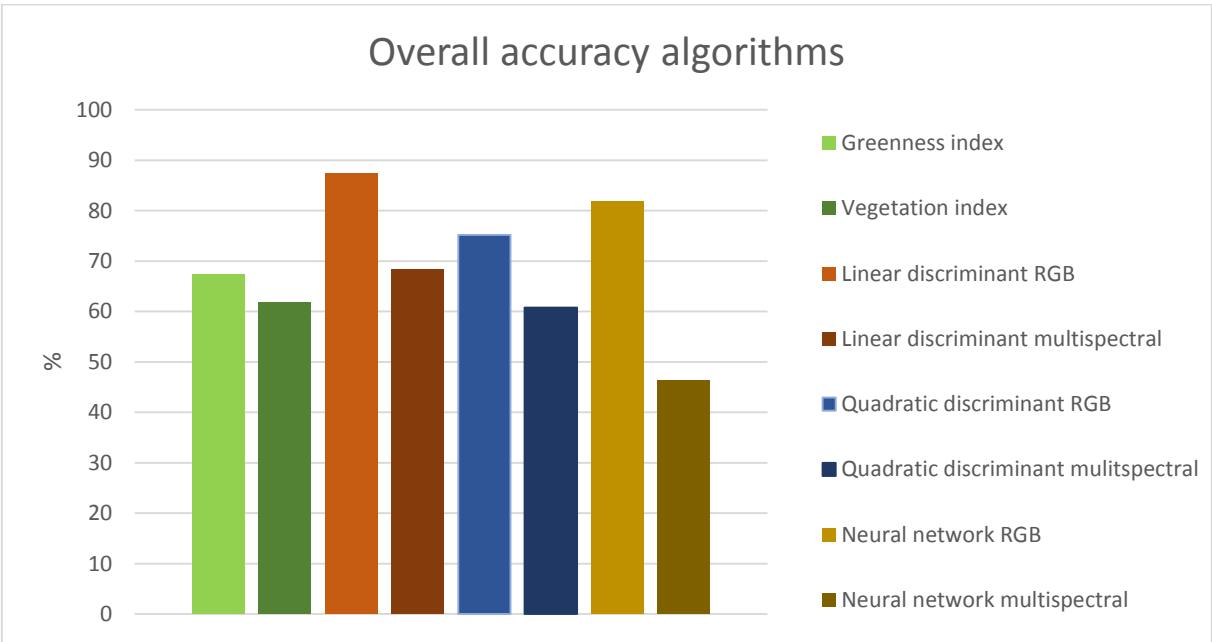
Figure 15. Overall accuracies of the used algorithms averaged for all validation samples for all fields

4.2   Training effect
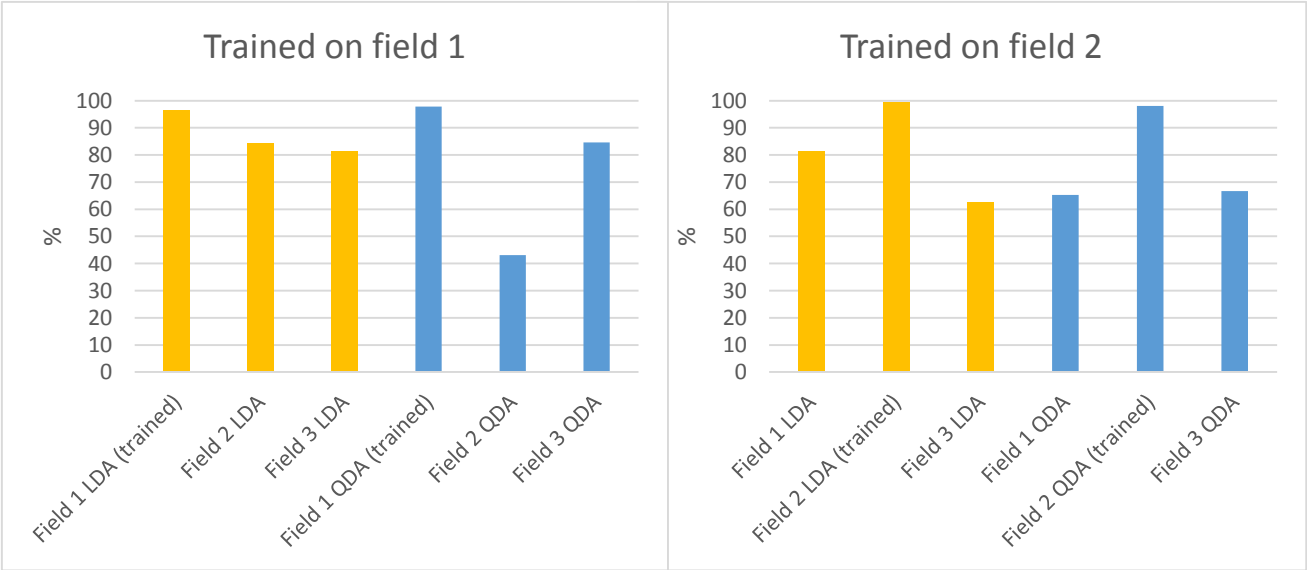
Figure 16. Effect of training on classification results

All of the tested algorithms show, for both the RGB images as the multispectral images, higher classification results for the validation half of field 1. To validate that this higher classification result is indeed caused by the fact that all algorithms have been trained on the same field, the LDA and QDA analysis have also been trained on field 2 (Figure 16). The LDA and QDA that were trained on field 1 performed quite poorly on field 2. However when trained on RGB images of one half of field 2 and validated on the other half of field 2 and the other fields, the results of field 2 become indeed much higher both compared to the earlier results of field 2 and compared to the other fields.

This indeed strongly suggests that training one of the used algorithms on a specific field makes that algorithm very successful in classifying another part of that same field on the same day. In other words, the used algorithms seem to be rather sensitive for changes in the circumstances.

4.3   Potential of hyperspectral images

To understand how much information is actually potentially embedded in the reflection of a certain patch one can look at the spectral signatures. A spectral signature visualises the recorded reflection as a function of the assessed wavelength. In Figure 17 the average signatures of all sugar beet patches, potato patches and soil patches in field 1 are depicted. Comparing the signature of the sugar beet patches to the potato patches mostly shows how similar those signatures are. The reflection from potato plants is more distributed than that of the sugar beet plants, especially in the NIR range. In general the potatoes also reflect more light. Yet between the reflection distributions coming from potato plants and sugar beet plants there remains a clear overlap. This explains that even when trained on a particular field those plants cannot always be clearly identified. The soil (sand) reflection of field 1 is much lower, especially in the NIR range, than the reflection of the plants. Separating the soil classes from the vegetation should therefore indeed be achievable.

For field 2 (Figure 18) the spectral reflection of sugar beet plants occurs to be both lower and in a smaller range compared to field 1. The reflection of the potato plants is also a bit lower but still widely distributed, especially in the NIR range. Again there is an overlap in reflection intensities measured from both plants. The soil (clay) reflection of field 2 looks rather similar to the soil reflection of field 1.

For field 3 (Figure 19) the spectral reflection intensities for the potato plants and sugar beet plants are higher than those of field 1 and 2 and not as widely distributed as in field 1. In this case the reflection signatures of the sugar beet plants and potato plants also seem to have very little overlap. The soil (sand) reflection increases much more with the higher wavelengths compared to the other fields.

The spectral signature of the soil patches is obviously very different from the sugar beet and potato patches. It therefore seems that identifying those patches should be relatively easy. This may explain why the accuracy of identifying soil patches was high for most of the tested algorithms.

Figure 17. Spectral signatures of Sugar beet, Potato and Soil patches on Field 1. The lines show the quartiles of the hyperspectral reflection. The boxplots show the reflection from the RGB images for Red, Green and Blue from right to left.

Figure 18. Spectral signatures of Sugar beet, Potato and Clay patches on field 2. The lines show the quartiles of the hyperspectral reflection. The boxplots show the reflection from the RGB images for Red, Green and Blue from right to left.
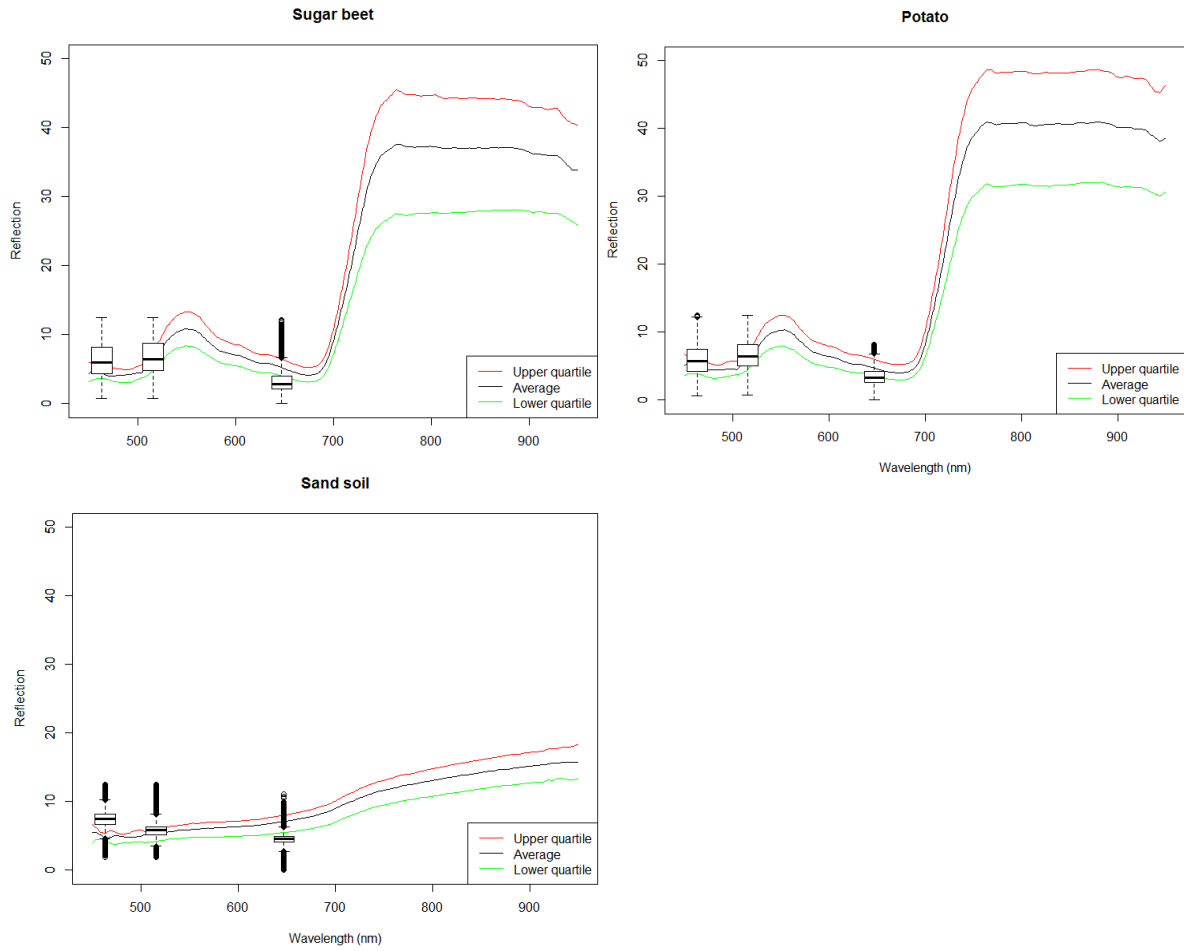

Figure 19. Spectral signatures of Sugar beet, Potato and Soil patches on Field 3. The lines show the quartiles of the hyperspectral reflection. The boxplots show the reflection from the RGB images for Red, Green and Blue from right to left.
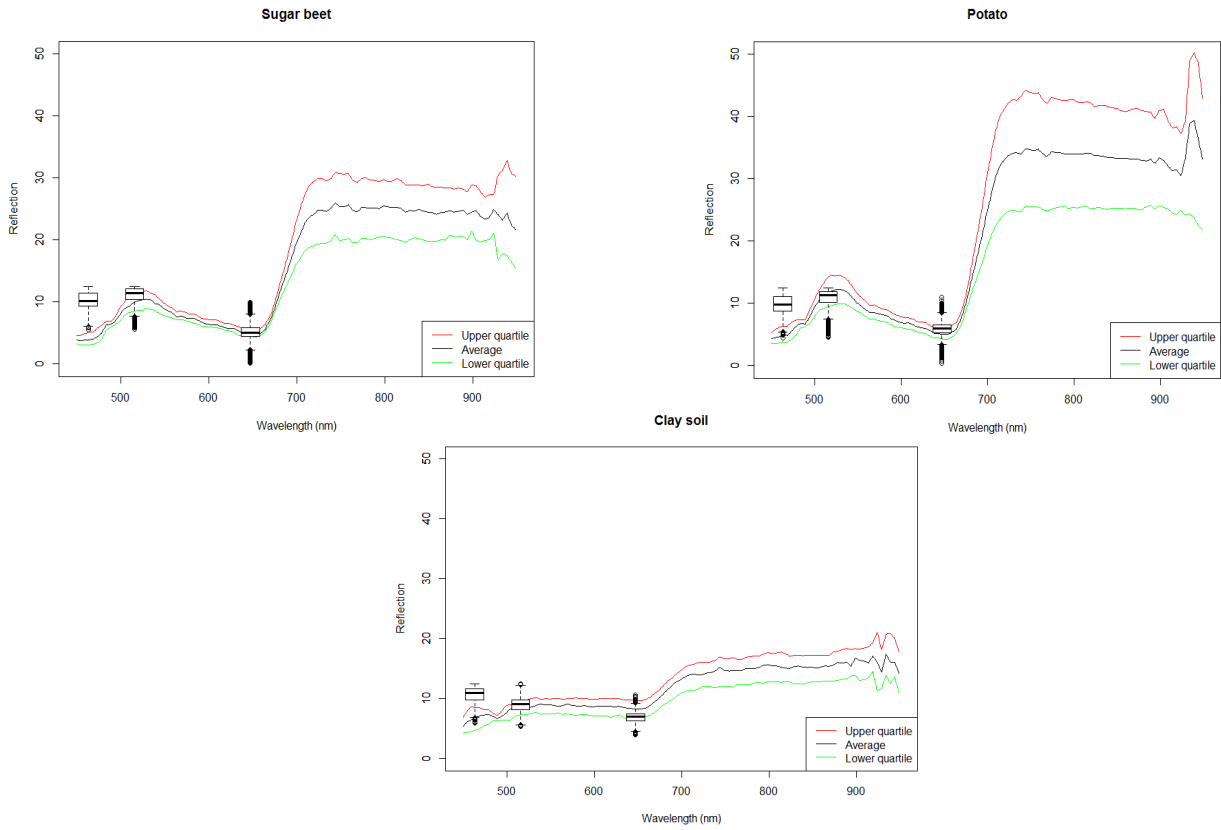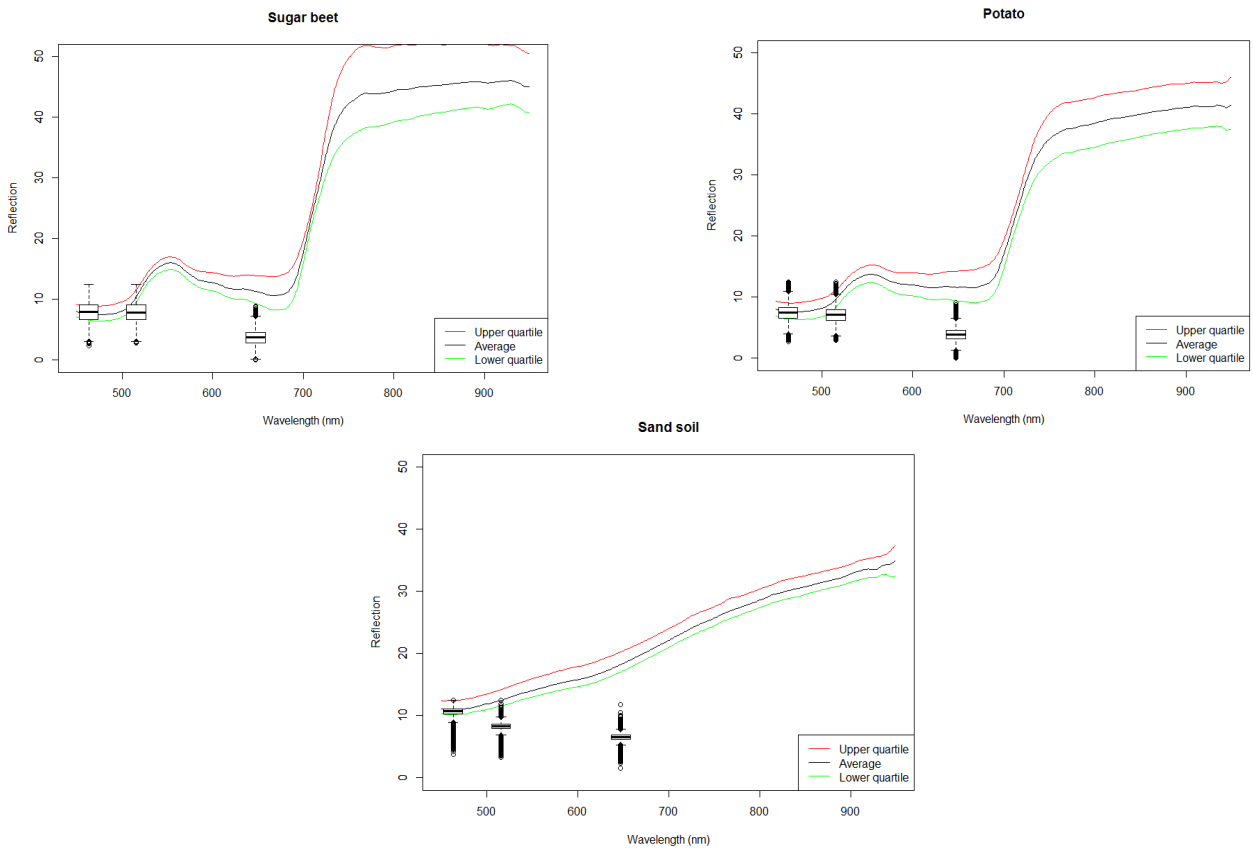
5 Discussion

5.1 Classification performance

The overall classification accuracies (Figure 15) show that none of the tested algorithms achieves a classification accuracy over 90%. Compared to classification accuracies achieved by UGVs (Table 1) those accuracies seem rather low. However when looking closer at the result of each classification algorithm it strikes that most of them, and especially the machine learning techniques, perform very well on field 1, which is the training field. Especially the ANN performs very well on field 1 with a classification accuracy of 99% averaged for all classes. Also the false negative percentage of the volunteer potatoes stays rather low with just 3%. This is especially low compared to most of the false negatives in the assessed literature (Slaughter et al 2008). The false positives for the volunteer potatoes is with 0% on field 1 also extremely low. That having said the, for field 2 and 3 the ANN achieves much lower classification accuracies and higher percentages of false positives and false negatives.

The other classification algorithms perform generally worse than the ANN. Especially the indices score low classification accuracies. The LDA on RGB images achieves the highest classification accuracy averaged over all 3 fields but performs worse than de ANN on field 1.

For all of the tested algorithms the classification algorithms perform much better on the training field, field 1, than on the other two fields. This suggest that the machine learning algorithms can be successfully trained for classification but are then not able to perform for images made under different conditions. This training effect also reveals itself when the LDA and QDA were trained on half of field 2 (Figure 16) which highly increased the classification accuracy for the other half of field 2 but led to a strongly decreased classification accuracies for field 1 and 3.

The identified training effect poses an obstacle towards the development of generically trained classification algorithms, i.e. trained classification algorithms that would achieve high classification accuracies under a variation of conditions. Such a generically trained classification algorithm would especially be applicable for UAVs that have to monitor weeds during different weather conditions and for different stages in the growing season.

To reduce the training effect one could assess the variables that can cause it and could possibly be compensated for.

5.1.1 Field conditions

The results of this study showed that most algorithms will perform much better on the field they are trained on than on other fields. This suggest that the field conditions during the recording of the images differ too much and have too much influence on the recorded reflection to train a classification algorithm in a way it is able to perform well without taking those differences of conditions into account. The differences between the fields included: different lengths of growing period, growing period in different times of the year, different atmospheric conditions during the image recording, image recording were performed on different times of the day, different soil compositions and different moisture contents of the soil. As for none of these differences the relationship to the measured reflection are known, and as none of these differences have been measured during the study, it is not possible to conclude which differences should be controlled in order to achieve a more generic classification.

5.1.2 Natural light source

The light source plays an important role in the measured reflection. First of all the intensity of the light source obviously is of influence on the total recorded reflection. This means that it matters how strong the sun is on the moment of recording. This influence has been partly taken into account by equalizing the white balance of all multispectral pictures by using a reference panel before every flight. During the flight however, the light conditions can also significantly change mostly due to overcoming clouds.

This disturbance in the intensity of the light source is hard to take into account and has likely decreased the quality of the images used during this study.

Secondly, the angle of the incoming light causes another challenge. With different angles of incoming light different patterns of shadows are formed. If those shadows fall on a certain patch, the reflection recorded from this patch is lowered. The identification of soil patches should not be too much of a problem since the expected reflection from soil is already much lower than from patches with plants. However when a shadow falls over a patch with potatoes or sugar beets this may cause a wrong identification of such a patch.

5.2   Classification strategy

On the RGB images it is possible for humans to visually distinguish the potatoes from the sugar beets and from the soil. This is partly because the human brain looks mainly to the structure and the form of an object (Tarr & Bülthoff 1998). Such a form of recognition is called object based classification and this possibility has not been explored in this study and should be of interest for further research, especially because visual structures are already often used in classification by UGV (Cho et al 2002, Shinde & Shukla 2014). That having said, it should be noted that object based recognition does demand a high enough resolution to identify specific structures of a plant. Since hyperspectral cameras have in principle very little room for increasing the resolution it seems that the potential of object based recognition is mostly in RGB images made on relatively low altitudes. For estimates of crop covers or weed fractions based on images taken from higher altitudes, object based classification is less likely to form a solution.

Another possible option for more accurate weed recognition is the use of prior information on the agricultural system. If for example the crop is planted in confined rows (as is the case with sugar beets) those rows can be identified. Plants deviating from such a row could then already be classified as very likely to be weeds before the classification starts.

Yet another option would be including other sensors on the UAV. Active sensors like a LiDAR can sense additional information on the plants like the height and structure and even create 3D models of the plants. Such an approach may be expected to achieve much higher identification accuracies. It should be taken into account that the computational demand for such systems will also be much higher and can potentially limit the possibility of real-time classification.

5.3   Use of multispectral images

Generally bands outside the visual part of the spectrum, particularly in the NIR wavelengths, are considered useful inputs for the recognition of vegetation (Anyamba & Tucker 2012). For the crop identification in this study the results show however that the tested algorithms all perform better at identifying the crop when only RGB images are used as input (Figure 15). This suggest that bands outside the visual spectra are redundant and may even be contra-effective when it comes to crop identification. When the complete reflection of the hyperspectral signatures was visualised (Figure 17, Figure 18 and Figure 19) the reflection range of sugar beets indeed show a significant overlap with the reflection range of the potatoes. This overlap was present both within the same field as between the reflection ranges of different fields. This overlap also indicates that using this reflection is not very suitable to make a distinction between sugar beet plants and potato plants.

Moreover, the spatial resolution is in principle much higher for RGB images than for hyperspectral images under the same circumstances. It therefore seems that RGB images do have a better prospect for identification of plant types.

5.4 Choice of bandwidths ranges

In this study both RGB images and multispectral images, created from hyperspectral images, were used as inputs for the crop classification algorithms. The conversion from hyperspectral images to multispectral images has been performed to reduce the computational demand for the used algorithms. The choice of bandwidth ranges has been based on the bandwidths ranges used on the RapidEye satellite (Table 4). There are, however, two concerns with the choice of those bandwidth ranges.

First of all, given that the original images included reflection intensities in the range from 450 nm to 950 nm, multispectral images consisting of different wavelengths or larger of smaller ranges would have been an option as well. Instead of taking predefined bandwidth ranges it would have been possible to determine a set of wavelengths ranges with the highest signal-to-noise ratio (Bajcsy & Groves 2004, Choi et al 2012). In doing so one does also not necessarily have to choose between using RGB images or hyperspectral images but instead could select the bands from both images that have the best classification prospects. No such pre-selection has performed in this study.

Secondly, the current multispectral images include a red-edge band. The reflection values of the red-edge band has been used as input to the classification algorithms along with the reflection values of the other bands. Some studies have however suggested that the plant specific information, mainly the chlorophyll intensity, does mostly correlate with the position of the red-edge, instead of the mean reflection value of the bandwidth range in which the red-edge occurs (Cho & Skidmore 2006). Since the hyperspectral information was available the location of the red-edge for the sugar beet class and the potato plant class could have been determined. In this study, however, the inputs have been used as a multispectral image and thus included a reflection value for the bandwidth range of the red-edge rather than the position of the red-edge itself.

5.5 Potential for future applications

Although this study shows that there are clearly a number of challenges weed detection by UAVs have to cope with, many of those challenges can potentially be met and higher detection accuracies should be perceived as achievable. In comparison to UAVs, however, it should be expected that ground vehicles will be able to achieve even higher accuracies in principle due to the closer proximity and the ability to control more environmental factors (Slaughter et al 2008). This suggests that agricultural deployed UAVs are not as likely to compete with UGVs. However there could be advantages of using both UGVs and UAVs in the same weed control system.

The benefits of using UAVs compared to UGVs is that UAVs can cover large areas in little time and they do not disturb the plants or soil. This means that for regular weed monitoring on large fields UAVs would have a definite advantage.

It is especially those qualities that make deploying an UGV and UAV at the same time an interesting option. By pre-identifying weeds in the field the UGV could work more efficient in terms of optimal path planning, only scanning plants likely to be weeds, or only entering parts of the field where weeds form an actual threat to the grown crop.

If optimal path planning is considered as an application there should also some thoughts be given to the communication between the deployed UAV and UGV. One option is that the UAV create an initial weed map that is then used by the UAV.

A more integrated approach could be a scenario in which the UAV executes real-time classification and uses the outcome to do some additional measurements on plants that may be weeds. The location of those plants could then, possibly in combination with a percentage of certainty, be passed down to the UGV which uses this information for its path planning. The classification of the UGV could then again be passed up to the UAV which can use this information to improve its own classification parameters.

A location in the latter scenario could consist of a coordinate in terms of a chosen coordinate system. However if the studied plot consists of rows of crops, one could consider to led the UAV recognize such

rows and pass the location of a potential weed in terms of a row number and a length into that row. This could assist the UGV in planning an optimal path through the field. Further research is recommended to identify the optimal set-up and implications for such a system.

5.6   Real-time identification

In this study a pre-processing chain was used before running the detection algorithms. This does not necessarily mean that real-time identification is an impossibility given the used apparatus and software especially when only the RGB images are being used. Where the hyperspectral images were both radiometrically calibrated and geometrically rectified, the RGB images were only mosaicked to form one picture. This is in principle an unnecessary step for real-time identification since the single images can immediately be used. Since the location of these images are known, identified plants on those images can automatically be given a coordinate.

The used algorithms in this study were all coded in R, which runs on almost every platform. In this case the UAV is controlled by a Raspberry Pi which certainly would also be able to read the images from the used camera and run R-scripts.

6 Conclusions and recommendations

The results of this study show that crop classification based on reflection is not only feasible but also already achievable with equipment and algorithms used in this study. Especially the machine learning techniques assessed in this study (LDA, QDA and ANN) performed very well with RGB images as input and when trained for specific field conditions, with the ANN reaching a classification accuracy of 99%. This study also showed that those machine learning techniques are condition sensitive. When the same ANN was validated for the two other fields, the classification accuracy drops to 71% and 75%. The same pattern is present for the other tested classification algorithms. This means that machine learning techniques trained under the conditions of a specific field will achieve high classification accuracies for that field but much lower accuracies for other fields. If the machine learning classifications methods described in this study were to be applied, field specific training should therefore be performed before the commence of any classification.

Using indices combined with optimal thresholds to classify different classes proofed to be unsuccessful.

This study found no advantage of using multispectral images over RGB images. Instead for all tested algorithms using RGB images resulted in a better classification performance. Analysing spectral signatures shows there is significant overlap in recorded reflections between the classes 'sugar beet plants' and 'potato plants'. This suggests that most of the recorded reflection by the hyperspectral camera may not be suitable for making a clear distinction between those classes. This, together with the lower spatial resolution may explain part of the lower classification accuracies when multispectral images are used. However, this study has also raised some concerns about the band choices for the creation of the multispectral images.

With weed recognition by UAVs proven to be a possibility, this study also briefly touched upon the potentials of involving UAVs in agricultural systems monitoring. One concern that has been discussed is the real-time identification of weeds. Looking at the pre-processing steps that have been executed in this study it could be concluded that processing hyperspectral images on board is likely to be too computational demanding with the current state of technology. However direct processing of RGB images seems to be well within the current capabilities and could be executed with exactly the same methods as used in this study. From a performance point of view the use of RGB images should also have the preference as the classification accuracies has proven to be higher than those resulting from multispectral images.

When UAVs would indeed be deployed to do real-time identification it is unlikely that they would also be used for executing any follow-up actions. Although the design of a weed detection and removal system is well beyond the scope of this study, it could be imagined that the UAV either triggers an action on the ground when the found weeds pass a certain threshold or coordinate an action on the ground. In the latter case the identification of weeds could for example help for optimal path planning of ground vehicles.

This study has also left a few important aspects of weed recognition by UAVs for further research:
- Using object classification instead of pure reflection to make a distinction between crops and weeds;
- Preselecting bands and determining band ranges from hyperspectral images and RGB images based on a methodology to find the highest signal-to-noise ratio;
- The development of automated weed control systems using UAVs and UGVs real-time in an integral system.

7 References

Anyamba A, Tucker CJ. 2012. Historical perspective of AVHRR NDVI and vegetation drought monitoring. *Remote Sensing of Drought: Innovative Monitoring Approaches*: 23

Bajcsy P, Groves P. 2004. Methodology for Hyperspectral Band Selection. *Photogrammetric Engineering & Remote Sensing* 70: 793-802

Barrientos A, Colorado J, Cerro Jd, Martinez A, Rossi C, et al. 2011. Aerial remote sensing in agriculture: A practical approach to area coverage and path planning for fleets of mini aerial robots. *Journal of Field Robotics* 28: 667-89

Cho MA, Skidmore AK. 2006. A new technique for extracting the red edge position from hyperspectral data: The linear extrapolation method. *Remote Sensing of Environment* 101: 181-93

Cho S, Lee D, Jeong J. 2002. AE—Automation and Emerging Technologies: Weed–plant Discrimination by Machine Vision and Artificial Neural Network. *Biosystems engineering* 83: 275-80

Choi S-I, Oh J, Choi C-H, Kim C. 2012. Input variable selection for feature extraction in classification problems. *Signal Processing* 92: 636-48

Crippen RE. 1990. Calculating the vegetation index faster. *Remote Sensing of Environment* 34: 71-3

Duke SO. 2005. Taking stock of herbicide-resistant crops ten years after introduction. *Pest management science* 61: 211-8

Ehsan S, McDonald-Maier KD. 2009. *On-board vision processing for small UAVs: Time to rethink strategy*. Presented at Adaptive Hardware and Systems, 2009. AHS 2009. NASA/ESA Conference on

Elvidge CD, Chen Z. 1995. Comparison of broad-band and narrow-band red and near-infrared vegetation indices. *Remote Sensing of Environment* 54: 38-48

Feyaerts F, Van Gool L. 2001. Multi-spectral vision system for weed detection. *Pattern Recognition Letters* 22: 667-74

Gerhards R, Christensen S. 2003. Real-time weed detection, decision making and patch spraying in maize, sugarbeet, winter wheat and winter barley. *Weed research* 43: 385-92

Ghazali KH, Mustafa MM, Hussain A. 2008. Machine vision system for automatic weeding strategy using image processing technique. *American-Eurasian Journal of Agricultural and Environmental Science* 3: 451-8

Glasbey CA, Mardia KV. 1998. A review of image-warping methods. *Journal of Applied Statistics* 25: 155-71

Goldburg RJ. 1992. Environmental concerns with the development of herbicide-tolerant plants. *Weed Technology*: 647-52

Hansen KD, Garcia Ruiz FJ, Kazmi W, Bisgaard M, la Cour-Harbo A, et al. 2013. *An Autonomous Robotic System for Mapping Weeds in Fields*. Presented at Intelligent Autonomous Vehicles Symposium 2013

Hemming J, Rath T. 2001. PA—Precision Agriculture: Computer-Vision-based Weed Identification under Field Conditions using Controlled Lighting. *Journal of Agricultural Engineering Research* 78: 233-43

Jafari A, Mohtasebi SS, Jahromi HE, Omid M. 2006. Weed detection in sugar beet fields using machine vision. *Int. J. Agric. Biol* 8: 602-5

Kazmi W, Bisgaard M, Garcia-Ruiz F, Hansen KD, la Cour-Harbo A. 2011. *Adaptive surveying and early treatment of crops with a team of autonomous vehicles*. Presented at European Conference on Mobile Robots

Kudsk P, Streibig J. 2003. Herbicides—a two-edged sword*. *Weed Research* 43: 90-102

Lamb D, Brown R. 2001. PA—Precision Agriculture: Remote-Sensing and Mapping of Weeds in Crops. *Journal of Agricultural Engineering Research* 78: 117-25

Lee WS, Slaughter D, Giles D. 1999. Robotic weed control system for tomatoes. *Precision Agriculture* 1: 95-113

Levidow L. 2001. Precautionary Uncertainty Regulating GM Crops in Europe. *Social studies of science* 31: 842-74

Levidow L, Boschert K. 2008. Coexistence or contradiction? GM crops versus alternative agricultures in Europe. *Geoforum* 39: 174-90

McQueen RJ, Garner SR, Nevill-Manning CG, Witten IH. 1995. Applying machine learning to agricultural data. *Computers and electronics in agriculture* 12: 275-93

Miller JR, Hare EW, Wu J. 1990. Quantitative characterization of the vegetation red edge reflectance 1. An inverted-Gaussian reflectance model. *International Journal of Remote Sensing* 11: 1755-73

Nieto HJ, Brondo M, Gonzalez J. 1968. Critical periods of the crop growth cycle for competition from weeds.

Nieuwenhuizen A, Hofstee J, Henten Ev, Steen S, Zande J. 2008. *Automated detection and spraying of volunteer potato plants in sugar beet fields*. Presented at 5th International Weed Science Congress (IWSC)(pp. 252e253). Vancouver, British Columbia, Canada

Nieuwenhuizen A, Tang L, Hofstee J, Müller J, Van Henten E. 2007. Colour based detection of volunteer potatoes as weeds in sugar beet fields using machine vision. *Precision Agriculture* 8: 267-78

Owen MD, Zelaya IA. 2005. Herbicide-resistant crops and weed resistance to herbicides. *Pest Management Science* 61: 301-11

Perez A, Lopez F, Benlloch J, Christensen S. 2000. Colour and shape analysis techniques for weed detection in cereal fields. *Computers and electronics in agriculture* 25: 197-212

Piron A, Van Der Heijden F, Destain M-F. 2011. Weed detection in 3D images. *Precision Agriculture* 12: 607-22

Pollack JB. 1990. Backpropagation is sensitive to initial conditions. *Complex Systems* 4: 269-80

Pudełko R, Kozyra J, Nieróbca P. 2008. Identification of the intensity of weeds in maize plantations based on aerial photographs. *Žemdirbystė= Agriculture* 95: 130-4

Radosevich SR, Ghersa CM, Comstock G. 1992. Concerns a weed scientist might have about herbicide-tolerant crops. *Weed Technology*: 635-9

Rango A, Laliberte A, Steele C, Herrick JE, Bestelmeyer B, et al. 2006. Using unmanned aerial vehicles for rangelands: current applications and future potentials. *Environmental Practice* 8: 159

Shelton A, Wyman J. 1980. Postharvest Potato Tuberworm Population Levels in Cull and Volunteer Potatoes, and Means for Control. *Journal of Economic Entomology* 73: 8-11

Shinde AK, Shukla MY. 2014. CROP DETECTION BY MACHINE VISION FOR WEED MANAGEMENT. *International Journal of Advances in Engineering & Technology* 7

Singh OV, Ghai S, Paul D, Jain RK. 2006. Genetically modified crops: success, safety assessment, and public concern. *Applied microbiology and biotechnology* 71: 598-607

Slaughter D, Giles D, Downey D. 2008. Autonomous robotic weed control systems: A review. *Computers and electronics in agriculture* 61: 63-78

Suomalainen J, Anders N, Iqbal S, Roerink G, Franke J, et al. 2014. A Lightweight Hyperspectral Mapping System and Photogrammetric Processing Chain for Unmanned Aerial Vehicles. *Remote Sensing* 6: 11013-30

Tarr MJ, Bülthoff HH. 1998. Image-based object recognition in man, monkey and machine. *Cognition* 67: 1-20

Thorp K, Tian L. 2004. A review on remote sensing of weeds in agriculture. *Precision Agriculture* 5: 477-508

Timmons F. 1970. A history of weed control in the United States and Canada. *Weed Science*: 294-307

Torres-Sánchez J, López-Granados F, De Castro AI, Peña-Barragán JM. 2013. Configuration and specifications of an unmanned aerial vehicle (UAV) for early site specific weed management. *PloS one* 8: e58210

Tyc G, Tulip J, Schulten D, Krischke M, Oxfort M. 2005. The RapidEye mission design. *Acta Astronautica* 56: 213-9

Venables WN, Ripley BD. 2002. *Modern applied statistics with S*: Springer

Vrindts E, De Baerdemaeker J, Ramon H. 2002. Weed detection using canopy reflection. *Precision Agriculture* 3: 63-80

Weisenburger DD. 1993. Human health effects of agrichemical use. *Human pathology* 24: 571-6

Westergaard-Nielsen A, Lund M, Hansen BU, Tamstorf MP. 2013. Camera derived vegetation greenness index as proxy for gross primary production in a low Arctic wetland area. *ISPRS Journal of Photogrammetry and Remote Sensing* 86: 89-99

Wright GC, Bishop GW. 1981. Volunteer potatoes as a source of potato leafroll virus and potato virus X. *American Potato Journal* 58: 603-9

Wynne B. 2001. Creating public alienation: expert cultures of risk and ethics on GMOs. *Science as culture* 10: 445-81

Xiang H, Tian L. 2011. Development of a low-cost agricultural remote sensing system based on an autonomous unmanned aerial vehicle (UAV). *Biosystems engineering* 108: 174-90

Zhang C, Kovacs JM. 2012. The application of small unmanned aerial systems for precision agriculture: a review. *Precision Agriculture* 13: 693-712

Zimdahl RL. 1980. Weed-crop competition: a review. *Weed-crop competition: A review*

Zimdahl RL. 2013. *Fundamentals of weed science*: Academic Press

Appendix A. Classification results (in percentages) of all algorithms

Classification results

Legend:			"= True positives (%)"	
			"= False positives (%)"	

Greenness index results

Input images:		RGB

Positive classification (averaged over 3 fields): **67** %

Field 1

		Results			Number of patches
Average positive classification (%) for field: **85**		Bare soil	Volunteer potato	Sugar beet	
Groundtruth	Bare soil	100	0	0	143
	Volunteer potato	3	90	8	39
	Sugar beet	0	33	67	156

Field 2

		Results			Number of patches
Average positive classification (%) for field: **67**		Bare soil	Volunteer potato	Sugar beet	
Groundtruth	Bare soil	100	0	0	70
	Volunteer potato	1	99	0	102
	Sugar beet	1	96	3	128

Field 3

		Results			Number of patches
Average positive classification (%) for field: **49**		Bare soil	Volunteer potato	Sugar beet	
Groundtruth	Bare soil	100	0	0	148
	Volunteer potato	0	47	53	212
	Sugar beet	7	93	0	489

Vegetation index

Input images:	Multispectral

Positive classification (averaged over 3 fields): 62 %

Field 1

		Results			Number of patches
Average positive classification (%) for field:	**77**	Bare soil	Volunteer potato	Sugar beet	
Groundtruth	Bare soil	99	NA	NA	143
	Volunteer potato	NA	62	NA	39
	Sugar beet	NA	NA	70	156

Field 2

		Results			Number of patches
Average positive classification (%) for field:	**57**	Bare soil	Volunteer potato	Sugar beet	
Groundtruth	Bare soil	71	NA	NA	70
	Volunteer potato	NA	0	NA	98
	Sugar beet	NA	NA	99	126

Field 3

		Results			Number of patches
Average positive classification (%) for field:	**52**	Bare soil	Volunteer potato	Sugar beet	
Groundtruth	Bare soil	100	NA	NA	148
	Volunteer potato	NA	0	NA	212
	Sugar beet	NA	NA	56	489

Linear discriminant analysis

Input images: RGB

Positive classification (averaged over 3 fields): 87 %

Field 1

		Results			
Average positive classification (%) for field:	**96**	Bare soil	Volunteer potato	Sugar beet	Number of patches
Groundtruth	Bare soil	100	0	0	143
	Volunteer potato	0	100	0	39
	Sugar beet	0	11	89	156

Field 2

		Results			
Average positive classification (%) for field:	**84**	Bare soil	Volunteer potato	Sugar beet	Number of patches
Groundtruth	Bare soil	100	0	0	70
	Volunteer potato	0	100	0	102
	Sugar beet	1	46	53	128

Field 3

		Results			
Average positive classification (%) for field:	**81**	Bare soil	Volunteer potato	Sugar beet	Number of patches
Groundtruth	Bare soil	100	0	0	148
	Volunteer potato	40	51	9	212
	Sugar beet	0	7	93	489

Input images:	Multispectral

Positive classification (averaged over 3 fields): 68 %

Field 1

		Results			Number of patches
Average positive classification (%) for field:	**94**	Bare soil	Volunteer potato	Sugar beet	
Groundtruth	Bare soil	99	0	1	143
	Volunteer potato	3	90	8	39
	Sugar beet	0	7	93	156

Field 2

		Results			Number of patches
Average positive classification (%) for field:	**53**	Bare soil	Volunteer potato	Sugar beet	
Groundtruth	Bare soil	57	43	0	70
	Volunteer potato	1	99	0	102
	Sugar beet	2	94	3	126

Field 3

		Results			Number of patches
Average positive classification (%) for field:	**58**	Bare soil	Volunteer potato	Sugar beet	
Groundtruth	Bare soil	100	0	0	148
	Volunteer potato	64	16	20	212
	Sugar beet	31	12	58	485

Quadratic discriminant analysis

Input images:	RGB

Positive classification (averaged over 3 fields):   75   %

Field 1

		Results			
Average positive classification (%) for field:	**98**	Bare soil	Volunteer potato	Sugar beet	Number of patches
Groundtruth	Bare soil	100	0	0	143
	Volunteer potato	0	100	0	39
	Sugar beet	0	6	94	156

Field 2

		Results			
Average positive classification (%) for field:	**43**	Bare soil	Volunteer potato	Sugar beet	Number of patches
Groundtruth	Bare soil	14	0	86	70
	Volunteer potato	0	93	7	102
	Sugar beet	1	77	22	128

Field 3

		Results			
Average positive classification (%) for field:	**85**	Bare soil	Volunteer potato	Sugar beet	Number of patches
Groundtruth	Bare soil	99	0	1	148
	Volunteer potato	8	55	36	212
	Sugar beet	0	1	99	489

Input images:	Multispectral

Positive classification (averaged over 3 fields): 61 %

Field 1

		Results			
Average positive classification (%) for field:	**94**	Bare soil	Volunteer potato	Sugar beet	Number of patches
Groundtruth	Bare soil	99	0	1	143
	Volunteer potato	3	95	3	39
	Sugar beet	1	12	88	156

Field 2

		Results			
Average positive classification (%) for field:	**36**	Bare soil	Volunteer potato	Sugar beet	Number of patches
Groundtruth	Bare soil	6	71	23	70
	Volunteer potato	0	100	0	102
	Sugar beet	0	99	1	126

Field 3

		Results			
Average positive classification (%) for field:	**53**	Bare soil	Volunteer potato	Sugar beet	Number of patches
Groundtruth	Bare soil	100	0	0	148
	Volunteer potato	65	18	17	212
	Sugar beet	38	22	40	485

Neural Network

Input images: RGB

Positive classification (averaged over 3 fields): 82 %

Field 1

Average positive classification (%) for field:	**99**	Results			Number of patches
		Bare soil	Volunteer potato	Sugar beet	
Groundtruth	Bare soil	100	0	0	143
	Volunteer potato	3	97	0	39
	Sugar beet	0	0	100	140

Field 2

Average positive classification (%) for field:	**71**	Results			Number of patches
		Bare soil	Volunteer potato	Sugar beet	
Groundtruth	Bare soil	100	0	0	70
	Volunteer potato	0	56	44	111
	Sugar beet	3	38	59	128

Field 3

Average positive classification (%) for field:	**75**	Results			Number of patches
		Bare soil	Volunteer potato	Sugar beet	
Groundtruth	Bare soil	100	0	0	148
	Volunteer potato	52	29	19	212
	Sugar beet	2	2	96	485

Input images:	Multispectral

Positive classification (averaged over 3 fields): 46 %

Field 1

		Results			Number of patches
Average positive classification (%) for field:	**75**	Bare soil	Volunteer potato	Sugar beet	
Groundtruth	Bare soil	89	0	11	143
	Volunteer potato	3	56	41	39
	Sugar beet	1	19	79	156

Field 2

		Results			Number of patches
Average positive classification (%) for field:	**33**	Bare soil	Volunteer potato	Sugar beet	
Groundtruth	Bare soil	0	0	100	70
	Volunteer potato	2	0	98	102
	Sugar beet	2	0	98	126

Field 3

		Results			Number of patches
Average positive classification (%) for field:	**31**	Bare soil	Volunteer potato	Sugar beet	
Groundtruth	Bare soil	35	0	65	148
	Volunteer potato	47	3	50	212
	Sugar beet	43	1	56	485